RESEARCH

SIMPLIFIED SPT PERFORMANCE-BASED ASSESSMENT OF LIQUEFACTION AND EFFECTS: *TASKS 1 AND 2*

Prepared For:

Utah Department of Transportation
Research Division

Submitted By:

Brigham Young University
Department of Civil and Environmental Engineering

Authored By:

Kevin W. Franke
Levi T. Ekstrom
Kristin J. Ulmer

Year 1, Quarter 1 Update Report for the TPF-5(296) Technical Advisory Committee
June 2014

udot.utah.gov
Utah Department of Transportation - Research Division
4501 South 2700 West - P.O. Box 148410 - SLC,UT 84114-8410

DISCLAIMER

The authors alone are responsible for the preparation and accuracy of the information, data, analysis, discussions, recommendations, and conclusions presented herein. The contents do not necessarily reflect the views, opinions, endorsements, or policies of the Utah Department of Transportation or the U.S. Department of Transportation. The Utah Department of Transportation makes no representation or warranty of any kind, and assumes no liability therefore.

ACKNOWLEDGMENTS

The authors acknowledge the Utah, Idaho, Montana, Alaska, South Carolina, and Connecticut Departments of Transportation for funding this research for pooled fund study TPF-5(296). The views and opinions presented in this report represent those of its authors, and may not represent those of the state agencies funding this research.

TECHNICAL REPORT ABSTRACT

1. Report No.	2. Government Accession No.	3. Recipient's Catalog No.
NA	NA	NA

4. Title and Subtitle SIMPLIFIED SPT PERFORMANCE-BASED ASSESSMENT OF LIQUEFACTION AND EFFECTS: *TASKS 1 AND 2*	5. Report Date June 2014 6. Performing Organization Code NA
7. Author(s) Kevin W. Franke, Levi T. Ekstrom, Kristin J. Ulmer	8. Performing Organization Report No. NA
9. Performing Organization Name and Address Brigham Young University Department of Civil and Environmental Engineering 368 Clyde Building Provo-UT 84602-4009	10. Work Unit No. 4206515D 11. Contract or Grant No. 148753
12. Sponsoring Agency Name and Address Utah Department of Transportation 4501 South 2700 West P.O. Box 148410 Salt Lake City, UT 84114-8410	13. Type of Report & Period Covered Year 1, Quarter 1 TAC Update March-May 2014 14. Sponsoring Agency Code PIC No. UT13.407

15. Supplementary Notes

Prepared in cooperation with the Utah Department of Transportation and the U.S. Department of Transportation, Federal Highway Administration

16. Abstract

The purpose of the research being performed is to provide the benefit of the full performance-based probabilistic earthquake hazard analysis, without requiring special software, training, and experience. To do this, simplified models of liquefaction triggering and lateral spread displacements that approximate the results of the full probabilistic analysis were developed. This report provides the derivation and validation of these simplified models, addressing Tasks 1 and 2 of the TPF-5(296) research contract.

These simplified procedures are based on retrieving a reference value from a hazard-targeted liquefaction parameter map and calculating site-specific correction factors to adjust the reference value to represent the parameter for the site-specific soil profile. Site-specific values calculated using the simplified method are compared to those calculated using a full probabilistic method for ten cities in the United States. The difference between the full and simplified procedures for both liquefaction triggering and lateral spread displacement models is shown to be within an acceptable amount. This shows that the simplified procedures derived in this report can reasonably approximate the results of a full probabilistic procedure.

17. Key Words		18. Distribution Statement		23. Registrant's Seal
Lateral Spread Displacements, Liquefaction Triggering, Performance-based Engineering Reference Maps, Simplified Models, Seismic Hazards		Not restricted. Available through: UDOT Research Division 4501 South 2700 West P.O. Box 148410 Salt Lake City, UT 84114-8410 www.udot.utah.gov/go/research		NA
19. Security Classification (of this report)	20. Security Classification (of this page)	21. No. of Pages	22. Price	
Unclassified	Unclassified	64	NA	

TABLE OF CONTENTS

LIST OF TABLES

LIST OF FIGURES

UNIT CONVERSION FACTORS

Units used in this report and not conforming to the UDOT standard unit of measurement (U.S. Customary system) are given below with their U.S. Customary equivalents:

SI* (MODERN METRIC) CONVERSION FACTORS

APPROXIMATE CONVERSIONS TO SI UNITS				
Symbol	**When You Know**	**Multiply By**	**To Find**	**Symbol**
		LENGTH		
in	inches	25.4	millimeters	mm
ft	feet	0.305	meters	m
yd	yards	0.914	meters	m
mi	miles	1.61	kilometers	km
		AREA		
in^2	square inches	645.2	square millimeters	mm^2
ft^2	square feet	0.093	square meters	m^2
yd^2	square yard	0.836	square meters	m^2
ac	acres	0.405	hectares	ha
mi^2	square miles	2.59	square kilometers	km^2
		VOLUME		
fl oz	fluid ounces	29.57	milliliters	mL
gal	gallons	3.785	liters	L
ft^3	cubic feet	0.028	cubic meters	m^3
yd^3	cubic yards	0.765	cubic meters	m^3
		NOTE: volumes greater than 1000 L shall be shown in m^3		
		MASS		
oz	ounces	28.35	grams	g
lb	pounds	0.454	kilograms	kg
T	short tons (2000 lb)	0.907	megagrams (or "metric ton")	Mg (or "t")
		TEMPERATURE (exact degrees)		
°F	Fahrenheit	5 (F-32)/9 or (F-32)/1.8	Celsius	°C
		ILLUMINATION		
fc	foot-candles	10.76	lux	lx
fl	foot-Lamberts	3.426	candela/m^2	cd/m^2
		FORCE and PRESSURE or STRESS		
lbf	poundforce	4.45	newtons	N
lbf/in^2	poundforce per square inch	6.89	kilopascals	kPa

APPROXIMATE CONVERSIONS FROM SI UNITS				
Symbol	**When You Know**	**Multiply By**	**To Find**	**Symbol**
		LENGTH		
mm	millimeters	0.039	inches	in
m	meters	3.28	feet	ft
m	meters	1.09	yards	yd
km	kilometers	0.621	miles	mi
		AREA		
mm^2	square millimeters	0.0016	square inches	in^2
m^2	square meters	10.764	square feet	ft^2
m^2	square meters	1.195	square yards	yd^2
ha	hectares	2.47	acres	ac
km^2	square kilometers	0.386	square miles	mi^2
		VOLUME		
mL	milliliters	0.034	fluid ounces	fl oz
L	liters	0.264	gallons	gal
m^3	cubic meters	35.314	cubic feet	ft^3
m^3	cubic meters	1.307	cubic yards	yd^3
		MASS		
g	grams	0.035	ounces	oz
kg	kilograms	2.202	pounds	lb
Mg (or "t")	megagrams (or "metric ton")	1.103	short tons (2000 lb)	T
		TEMPERATURE (exact degrees)		
°C	Celsius	1.8C+32	Fahrenheit	°F
		ILLUMINATION		
lx	lux	0.0929	foot-candles	fc
cd/m^2	candela/m^2	0.2919	foot-Lamberts	fl
		FORCE and PRESSURE or STRESS		
N	newtons	0.225	poundforce	lbf
kPa	kilopascals	0.145	poundforce per square inch	lbf/in^2

*SI is the symbol for the International System of Units. (Adapted from FHWA report template, Revised March 2003)

LIST OF ACRONYMS

EDP	Engineering Demand Parameter
FHWA	Federal Highway Administration
GMPE	Ground Motion Predictive Equation
IM	Intensity Measure
PBEE	Performance-Based Earthquake Engineering
PSHA	Probabilistic Seismic Hazard Analysis
UDOT	Utah Department of Transportation

LIST OF TERMS

Liquefaction Triggering Terms

a_{max}	peak ground surface acceleration
CRR	cyclic resistance ratio
$CRR_{PL=50\%}$	median CRR (CRR corresponding to a probability of liquefaction of 50%)
CSR	cyclic stress ratio
CSR^{ref}	uniform hazard estimate of CSR associated with the reference soil profile
CSR^{site}	site-specific uniform hazard estimate of CSR
ΔCSR_{σ}	correction factor for vertical stress
ΔCSR_{Fpga}	correction factor for soil amplification
ΔCSR_{rd}	correction factor for shear stress reduction
ΔCSR_{MSF}	correction factor for magnitude scaling factor
$\Delta CSR_{K\sigma}$	correction factor for overburden pressure
ΔCSR	difference between CSR^{site} and CSR^{ref} values
FC	fines content (%)
FS_L	factor of safety against liquefaction triggering
FS_L^{site}	site-specific uniform hazard estimate of FS_L
F_{PGA}	soil amplification factor
K_{σ}	overburden correction factor (Idriss and Boulanger model)
MSF	magnitude scaling factor
M_w	mean moment magnitude
N	SPT blow count (uncorrected)
$(N_1)_{60}$	SPT resistance corrected to 60% efficiency and 1 atm pressure
$(N_1)_{60,cs}$	clean sand-equivalent SPT corrected to 60% efficiency and 1 atm pressure
N_{req}	SPT resistance required to resist or prevent liquefaction
N_{req}^{ref}	uniform hazard estimate of N_{req} associated with the reference soil profile
N_{req}^{site}	site-specific uniform hazard estimate of N_{req}
ΔN_L	difference between N_{site} and N_{req} values
P_a	atmospheric pressure (1 atm, 101.3 kPa, 0.2116 psf)
PGA	peak ground acceleration
P_L	probability of liquefaction
r_d	shear stress reduction coefficient
SPT	Standard Penetration Test
$V_{s,12}$	average shear wave velocity in upper 12 m (39.37 ft) of soil profile
z	depth to middle of soil profile layer
γ	unit weight of soil (i.e. pcf, kN/m^3, etc.)
σ_{ε}	error term for either model + parametric uncertainty or parametric uncertainty
σ_T	error term for both model and parametric uncertainty

σ_v	total vertical stress in the soil
σ'_v	effective vertical stress in the soil
Λ_{FSL*}	mean annual rate of not exceeding some given value of FS_L
λ_{Nreq*}	mean annual rate of not exceeding some given value of N_{req}
τ_{cyc}	equivalent uniform cyclic shear stress
Φ	standard normal cumulative distribution function

Lateral Spread Displacement Terms

D_H	median computed permanent lateral spread displacement (m)
R	closest horizontal distance from the site to the source (km)
M	earthquake moment magnitude
W	free-face ratio (%)
S	ground slope (%)
T_{15}	cumulative thickness (in upper 20 m) of all saturated soil layers with corrected SPT blowcounts (i.e., $(N_1)_{60}$) less than 15 blows/foot (m)
F_{15}	average fines content of the soil comprising T_{15} (%)
$D50_{15}$	average mean grain size of the soil comprising T_{15} (mm)
$\mathscr{L}$	Loading Parameter
$\mathscr{S}$	Site Parameter
$\mathscr{D}$	transformed (e.g. log, ln, square root) lateral spread displacement
ε	uncertainty term (used in lateral spread displacement model)
$\left[\log D_H\right]^{site}$	logarithm of the lateral spread displacement adjusted for site-specific conditions
$\left[\log D_H\right]^{ref}$	logarithm of the lateral spread displacement corresponding to the reference site
ΔD_H	adjustment factor for lateral spread displacement
D_H^{site}	site-specific hazard-targeted lateral spread displacement

EXECUTIVE SUMMARY

The purpose of the research being performed is to provide the benefit of the full performance-based probabilistic earthquake hazard analysis, without requiring special software, training, and experience. To do this, simplified models of liquefaction triggering and lateral spread displacements that approximate the results of the full probabilistic analysis were developed. These simplified methods are designed to require only a few calculations programmed into a spreadsheet and a provided liquefaction parameter map. This report provides the derivation and validation of these simplified models, addressing Tasks 1 and 2 of the TPF-5(296) research contract.

The simplified procedure using the Boulanger and Idriss (2012) probabilistic liquefaction triggering model is derived based on principles from the Mayfield et al. (2010) derivation of the simplified procedure for the Cetin et al. (2004) probabilistic liquefaction triggering model. The new simplified procedure is based on retrieving a reference seismic loading value (i.e. CSR^{ref} (%)) from a hazard-targeted liquefaction parameter map, and calculating site-specific correction factors to adjust the reference value to represent the site-specific seismic loading (i.e. CSR^{site}). This site-specific value can be used to calculate factor of safety against liquefaction, FS_L, probability of liquefaction, P_L, and SPT resistance required to prevent liquefaction initiation, N_{req}. Values of N_{req} and FS_L calculated using the simplified method are compared to those calculated using a full probabilistic method for ten cities in the United States. The difference between the two procedures is shown to be within an acceptable amount (within 3.41% on average). This shows that the simplified procedure reasonably approximates the results of a full probabilistic procedure without requiring the use of special software, training and experience.

The simplified procedure for predicting lateral spread displacements is derived based on the Youd et al. (2002) empirical model. This simplified procedure involves retrieving a reference value for lateral spread displacement (i.e. $[\log D_H]^{ref}$) from a hazard-targeted parameter map and calculating the site-specific correction factor (i.e. ΔD_H) to adjust the reference value to represent the actual lateral spread displacement at the site (i.e. D_H^{site}). Values of D_H^{site} were calculated using the simplified method and compared to values of D_H^{site} calculated using a full probabilistic method for ten cities in the United States. The simplified procedure was shown to be a reasonable approximation of the full probabilistic procedure.

1.0 INTRODUCTION

1.1 Problem Statement

The purpose of the research being performed is to provide the benefit of the full performance-based probabilistic earthquake hazard analysis, without requiring special software, training, and experience. To do this, simplified models of liquefaction triggering and lateral spread displacements were developed that approximate the results of the full probabilistic analysis. The simplified models need to be validated to ensure that the simplified models provide results that adequately approximate the results from full performance-based model at a given return period.

1.2 Objectives

The objective of this report is to introduce the original models used to determine the earthquake hazards (i.e. liquefaction triggering and lateral spread displacement), provide in-depth derivations that demonstrate the development of the simplified methods, and then validate the simplified models by performing a site-specific analysis for several different sites using the simplified and full models, addressing Tasks 1 and 2 of the TPF-5(296) research contract.

1.3 Scope

The tasks to be performed in this research will be: deriving the simplified models, performing site-specific earthquake hazard analysis using the simplified and full models, and comparing the site-specific hazards to determine how closely the simplified model approximates the full model.

1.4 Outline of Report

The research conducted for this report will contain the following:

- Introduction
- Derivation of the Simplified Models
- Validation of the Simplified Models

- Conclusions
- Appendices

2.0 DERIVATION OF THE SIMPLIFIED MODELS

2.1 Overview

This section describes the derivation of the simplified liquefaction triggering and lateral spread displacement models. The original models will be introduced and the derivation process for the simplified models will be described in detail.

2.2 Performance-based Liquefaction Triggering Evaluation

This section will provide the necessary background to understand the simplified performance-based liquefaction triggering procedure. A brief discussion regarding empirical liquefaction triggering models will be provided, followed by a discussion of performance-based implementation of those models.

2.2.1 Empirical Liquefaction Triggering Models

While the use of liquefaction hazard maps can provide a useful preliminary assessment of liquefaction hazard for a site, most professionals rely upon site-specific liquefaction triggering assessment for use in design. One of the most widely used methods of assessment in engineering practice today is the simplified empirical procedure (Seed and Idriss 1971; Seed 1979; Seed and Idriss 1982; and Seed et al. 1985). According to this simplified procedure, liquefaction triggering is evaluated by comparing the seismic loading of the soil to the soil's resistance to liquefaction triggering. Seismic loading is typically characterized using a cyclic stress ratio, *CSR*, which is computed as:

$$CSR = \frac{\tau_{cyc}}{\sigma_v'} = 0.65 \frac{a_{\max}}{g} \frac{\sigma_v}{\sigma_v'} r_d \qquad (1)$$

where τ_{cyc} is the equivalent uniform cyclic shear stress, σ_v' is the effective vertical stress in the soil, $a_{\max}/g$ is the peak ground surface acceleration as a fraction of gravity, σ_v is the total vertical stress in the soil, and r_d is a shear stress reduction coefficient.

Soil resistance to liquefaction triggering is characterized by performing some in-situ soil test (e.g., standard penetration resistance, cone penetration resistance, shear wave velocity, etc.) and comparing its results to those from documented case histories of liquefaction triggering. Based on observation and/or statistical regression, a function for the in-situ test can be delineated that separates the "liquefaction" case histories from the "non-liquefaction" case histories. This delineated boundary is referred to as the cyclic resistance ratio, *CRR*, and represents the unique combinations of *CSR* and in-situ soil test values at which liquefaction triggers.

Engineers and geologists commonly quantify liquefaction triggering using a factor of safety against liquefaction triggering, FS_L. This parameter is calculated as:

$$FS_L = \frac{\text{Resistance}}{\text{Loading}} = \frac{CRR}{CSR} \tag{2}$$

Kramer and Mayfield (2007) and Mayfield et al. (2010) introduced an alternative method to quantifying liquefaction triggering. If using the standard penetration test (SPT), then *CRR* is a function of $(N_1)_{60-cs}$, which is the clean sand-equivalent, corrected SPT resistance for the soil layer. However, for a given level of seismic loading (i.e., *CSR*), the SPT resistance required to resist or prevent liquefaction, N_{req}, can be back-calculated from the *CRR* function. This term N_{req} can be used to compute FS_L using a modified form of Equation (2) as:

$$FS_L = \frac{CRR}{CSR} = \frac{CRR\left((N_1)_{60-cs}\right)}{CRR\left(N_{req}\right)} \tag{3}$$

where $CRR(N)$ denotes that *CRR* is a function of given value of SPT resistance, *N*.

Mayfield et al. (2010) defined the relationship between the actual SPT resistance for the given layer, N_{site}, and N_{req} as:

$$\Delta N_L = N_{site} - N_{req} \tag{4}$$

The relationship between *CSR*, *CRR*, N_{site}, and N_{req} is shown graphically in Figure 2.1, after Mayfield et al. (2010).

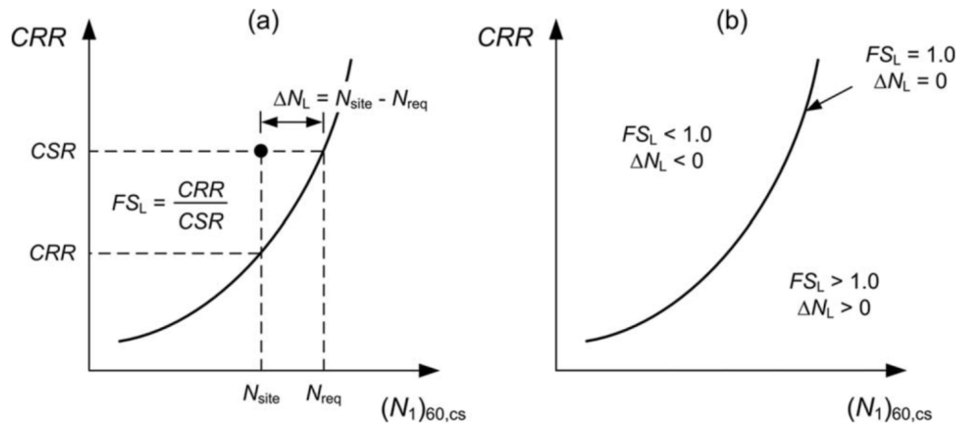

Figure 2.1 Schematic illustration of: (a) definitions of FS_L and ΔN_L; (b) relationship between FS_L and ΔN_L (after Mayfield et al. 2010)

2.2.2 Performance-based Liquefaction Triggering Assessment

Simplified empirical liquefaction triggering procedures require the selection of seismic loading parameters (i.e., peak ground surface acceleration a_{max} and moment magnitude M_w) to characterize a representative or design earthquake. When analyzing the liquefaction hazard from a single seismic source, the process of selecting seismic loading parameters is relatively straight-forward and simple. However, few seismic environments exist where only a single seismic source can contribute to liquefaction hazard. In more complex seismic environments, seismic hazard is usually calculated with a probabilistic seismic hazard analysis (PSHA), which often produces a wide range of seismic loading parameter combinations, each associated with a different likelihood of occurrence. Despite the wide variety of possible seismic loading parameter combinations produced by a PSHA, engineers must select a single set of seismic loading parameters that adequately characterize the complex seismicity of the site. Conventional approaches to liquefaction triggering assessment typically utilize the deaggregation results associated with the PSHA for a_{max} at a targeted hazard level or return period to obtain that single set of seismic loading parameters. Engineers select either the median or mean moment magnitude from the deaggregation results, and subsequently couple this selected magnitude with the a_{max} value associated with the targeted return period. Unfortunately, these conventional approaches were shown by Kramer and Mayfield (2007) to introduce bias into the computed liquefaction triggering hazard.

Potential biases introduced into the liquefaction triggering assessment through the improper and/or incomplete utilization of probabilistic ground motions and liquefaction triggering models could be reduced through the implementation of a performance-based approach (Franke et al. 2014a). Kramer and Mayfield (2007) presented such an approach, which utilized the probabilistic framework for performance-based earthquake engineering (PBEE) developed by the Pacific Earthquake Engineering Research Center (Cornell and Krawinkler 2000; Krawinkler 2002; Deierlein et al. 2003). This implementation of the PEER PBEE framework assigned the joint occurrence of M_w and $a_{\max}$ as an intensity measure, and either FS_L or N_{req} as the engineering demand parameter.

Kramer and Mayfield (2007) demonstrated that a hazard curve for FS_L could be developed using the following relationship:

$$\Lambda_{FS_L^*} = \sum_{j=1}^{N_M} \sum_{i=1}^{N_{a_{\max}}} P\left[FS_L < FS_L^* \mid a_{\max_i}, m_j\right] \Delta\lambda_{a_{\max_i}, m_j} \tag{5}$$

where $\Lambda_{FS_L^*}$ is the mean annual rate of *not* exceeding some given value of factor of safety, FS_L^*; $P\left[FS_L < FS_L^* \mid a_{\max_i}, \mathrm{m}_j\right]$ is the conditional probability that the actual factor of safety is less than FS_L^* given peak ground surface acceleration $a_{\max_i}$ and moment magnitude m_j; $\Delta\lambda_{a_{\max_i}, m_j}$ is the incremental joint mean annual rate of exceedance for $a_{\max_i}$ and m_j; and N_M and $N_{a_{\max}}$ are the number of magnitude and peak ground acceleration increments into which the intensity measure "hazard space" is subdivided.

The conditional probability component of Equation (5) can be solved with any selected probabilistic liquefaction triggering relationship, but that relationship must be manipulated to compute the desired probability. Assuming the inclusion of parametric uncertainty (i.e., uncertainty in SPT resistance and seismic loading), Kramer and Mayfield (2007) solved the conditional probability term using the Cetin et al. (2004) liquefaction triggering relationship as:

$$P\left[FS_L < FS_L^* \mid a_{\max_i}, m_j\right] = \Phi\left[-\frac{(N_1)_{60}(1+0.004FC) - 13.79\left(FS_L^* \cdot CSR_i\right) - 29.06\ln\left(m_j\right) - 3.82\ln\left(\frac{\sigma_v'}{p_a}\right) + 0.06FC + 15.25}{4.21}\right] \quad (6)$$

where Φ represents the standard normal cumulative distribution function, $(N_1)_{60}$ is the SPT resistance corrected for atmospheric pressure and hammer energy as computed using Cetin et al. (2004); FC is the fines content (in percent); CSR_i is equal to Equation (1) using $a_{\max_i}$ as in input; and p_a is atmospheric pressure (in the same units as σ_v').

Franke et al. (2014b) solved the conditional probability component of Equation (5) using the Boulanger and Idriss (2012) probabilistic liquefaction triggering relationship as:

$$P\left[FS_L < FS_L^* \mid a_{\max,i}, m_j\right] = \Phi\left[-\frac{\frac{(N_1)_{60,cs}}{14.1} + \left(\frac{(N_1)_{60,cs}}{126}\right)^2 - \left(\frac{(N_1)_{60,cs}}{23.6}\right)^3 + \left(\frac{(N_1)_{60,cs}}{25.4}\right)^4 - 2.67 - \ln\left(CSR_{i,j} \cdot FS_L^*\right)}{\sigma_\varepsilon}\right] \quad (7)$$

$$CSR_{i,j} = 0.65\frac{a_{\max,i}}{g}\frac{\sigma_v}{\sigma_v'}\left(r_d\right)_j\frac{1}{\left(MSF\right)_j}\frac{1}{K_\sigma} \quad (8)$$

where $(N_1)_{60}$ is the SPT resistance corrected for atmospheric pressure and hammer energy as computed using Idriss and Boulanger (2008, 2010); $(MSF)_j$ is the magnitude scaling factor for magnitude m_j and is computed according to Idriss and Boulanger (2008); $(r_d)_j$ is the depth reduction factor for magnitude m_j and is computed according to Idriss and Boulanger (2008); K_σ the depth correction factor and is computed according to Idriss and Boulanger (2008), and σ_ε is equal to either 0.13 for model uncertainty alone or 0.277 for total (i.e., model + parametric) uncertainty.

Similar to the relationship for computing a hazard curve for FS_L, Kramer and Mayfield (2007) derived a relationship for computing a hazard curve for N_{req} as:

$$\lambda_{N_{req}^*} = \sum_{j=1}^{N_M} \sum_{i=1}^{N_{a_{\max}}} P\left[N_{req} > N_{req}^* \mid a_{\max_i}, m_j\right] \Delta\lambda_{a_{\max_i}, m_j} \tag{9}$$

where $\lambda_{N_{req}^*}$ is the mean annual rate of exceeding some given clean sand-equivalent required SPT resistance, N_{req}^*, and $P\left[N_{req} > N_{req}^* \mid a_{\max_i}, \mathrm{m}_j\right]$ is the conditional probability that the actual N_{req} is greater than N_{req}^* given peak ground surface acceleration $a_{\max_i}$ and moment magnitude m_j. Kramer and Mayfield (2007) and Mayfield et al. (2010) used the Cetin et al. (2004) probabilistic liquefaction triggering relationship (assuming the inclusion of parametric uncertainty) to solve the conditional probability component of Equation (9) as:

$$P\left[N_{req} > N_{req}^* \mid a_{\max_i}, m_j\right] = \Phi\left[-\frac{N_{req}^* - 13.79\left(CSR_i\right) - 29.06\ln\left(m_j\right) - 3.82\ln\left(\dfrac{\sigma_v'}{p_a}\right) + 15.25}{4.21} \right] \tag{10}$$

Franke and Wright (2013) substituted the Boulanger and Idriss (2012) model for the Cetin et al. (2004) model to develop an alternative conditional probability term for Equation (9) as:

$$P\left[N_{req} > N_{req}^* \mid a_{\max,i}, m_j\right] = \Phi\left[-\frac{\dfrac{N_{req}^*}{14.1} + \left(\dfrac{N_{req}^*}{126}\right)^2 - \left(\dfrac{N_{req}^*}{23.6}\right)^3 + \left(\dfrac{N_{req}^*}{25.4}\right)^4 - 2.67 - \ln CSR_{i,j}}{\sigma_\varepsilon} \right] \tag{11}$$

where $CSR_{i,j}$ is computed with Equation (8), and σ_ε is equal to either 0.13 for model uncertainty alone or 0.277 for total (i.e., model + parametric) uncertainty.

2.3 Simplified Liquefaction Triggering Model

The Kramer and Mayfield (2007) performance-based liquefaction triggering procedure summarized in Section 2.2.2 is an effective solution to mitigating the deficiencies introduced by the conventional liquefaction triggering approach, which utilizes probabilistic ground motions and a liquefaction triggering relationship in a deterministic manner. Unfortunately, the Kramer and Mayfield procedure is relatively sophisticated and difficult for many engineers and geologists to apply in a practical manner. Specialized computational tools such as *WSliq* (Kramer 2008) and *PBliquefY* (Franke et al. 2014c) have been developed to assist these professionals in implementing the performance-based procedure. However, even the availability of computational tools is not sufficient for many professionals, who routinely need to perform and/or validate liquefaction triggering hazard calculations in a rapid and efficient manner.

An ideal solution to this dilemma would be the introduction of a new liquefaction analysis procedure that combined the simplicity and user-friendliness of traditional liquefaction hazard maps with the flexibility and power of a site-specific performance-based liquefaction triggering analysis. Mayfield et al. (2010) introduced such a procedure, which was patterned after the map-based procedure used in most seismic codes and provisions for developing probabilistic ground motions for engineering design. Franke et al. (2014d) later refined the Mayfield et al. simplified procedure for easier implementation in seismic codes and provisions.

Mayfield et al. (2010) demonstrated with the Cetin et al. (2004) liquefaction model that probabilistic estimates of liquefaction resistance (i.e. N_{req}) can be computed for a reference soil profile across a grid of locations to develop contour plots called liquefaction parameter maps. A liquefaction parameter map incorporating N_{req} can be a useful tool to evaluate the seismic demand for liquefaction at a given return period because N_{req} is directly related to *CSR* (i.e. Figure 2.1). Mayfield et al. demonstrated how these mapped "reference" values of N_{req} could be adjusted for site-specific conditions and used to develop site-specific uniform hazard estimates of N_{req} (i.e., N_{req}^{site}) and/or FS_L (i.e., FS_L^{site}) at the targeted return period or hazard level. The derivation of the simplified method for the Cetin et al. (2004) liquefaction triggering model will not be included in this report, but is presented in detail in Mayfield et al. (2010) and Franke et al. (2014d).

Because many engineers desire to evaluate liquefaction initiation hazard using either the Youd et al. (2001) or the Idriss and Boulanger (2006, 2008) (which is very similar to Youd et al. 2001) liquefaction triggering curves for the SPT, a simplified uniform hazard liquefaction procedure that incorporates the Boulanger and Idriss (2012) probabilistic liquefaction model can be developed through an approach similar to that used by Mayfield et al. (2010).

2.3.1 Simplified Procedure Using the Boulanger and Idriss (2012) Probabilistic Liquefaction Triggering Model

According to the probabilistic liquefaction triggering relationship developed by Boulanger and Idriss (2012), the probability of liquefaction P_L is given as:

$$P_L = \Phi\left[-\frac{\ln\left(CRR_{P_L=50\%}\right) - \ln\left(CSR\right)}{\sigma_T}\right] \tag{12}$$

where Φ represents the standard normal cumulative distribution function, σ_T is the total uncertainty of the liquefaction model, and $CRR_{P_L=50\%}$ is the cyclic resistance ratio corresponding to a probability of liquefaction of 50% (i.e. median *CRR*), which is computed as:

$$CRR_{P_L=50\%} = \exp\left[\left(\frac{(N_1)_{60,cs}}{14.1}\right) + \left(\frac{(N_1)_{60,cs}}{126}\right)^2 - \left(\frac{(N_1)_{60,cs}}{23.6}\right)^3 + \left(\frac{(N_1)_{60,cs}}{25.4}\right)^4 - 2.67\right] \tag{13}$$

Unlike the Mayfield et al. (2010) simplified liquefaction procedure, which incorporates the Cetin et al. (2004) liquefaction model, the simplified uniform hazard liquefaction procedure for the Boulanger and Idriss (2012) liquefaction model cannot be derived to solve for N_{req}^{site} in a convenient manner because of the 4th-order polynomial equation in *CRR* (i.e. Equation (13)). Fortunately, this simplified procedure can be modified to incorporate *CRR* and *CSR* instead of N_{req}, which greatly simplifies the derivation of the new procedure, and also makes it somewhat more intuitive.

Figure 2.2 presents a generic soil profile representing a reference site originally introduced by Mayfield et al. (2010) and used for the simplified Cetin et al. (2004) procedure. This reference soil profile can be used with a full performance-based liquefaction analysis incorporating the Boulanger and Idriss (2012) probabilistic liquefaction model (Franke and Wright 2013) to find N_{req} at a depth of 6 meters for the targeted return period (T_R) or hazard level. Because the value of N_{req} associated with the reference soil profile does not represent any actual soil profile, Mayfield et al. (2010) distinguished it using the term N_{req}^{ref}. By substituting N_{req}^{ref} into Equation (13), the median *CSR* associated with the reference site (i.e. CSR^{ref}) at the targeted return period can be computed. In other words, CSR^{ref} represents a uniform hazard estimate of the seismic loading that must be overcome to prevent liquefaction triggering if the reference soil profile existed at the site of interest. By computing similar hazard-targeted values of CSR^{ref} at different locations across a geographic area, contoured liquefaction parameter maps for CSR^{ref} can be constructed. These maps will be called *liquefaction loading maps* because they convey information regarding the seismic loading affecting liquefaction triggering, and to distinguish them from liquefaction parameter maps, which convey information regarding N_{req}^{ref}. Because *CSR* is often a decimal value less than unity, mapping the percent of *CSR*, $CSR^{ref}(\%)$ allows for more precise contour mapping, as well as easier interpretation and interpolation for design engineers. Figure 2.3 presents a liquefaction loading map of $CSR^{ref}(\%)$ at a return period of 1,033 years for a portion of the Salt Lake Valley in Utah.

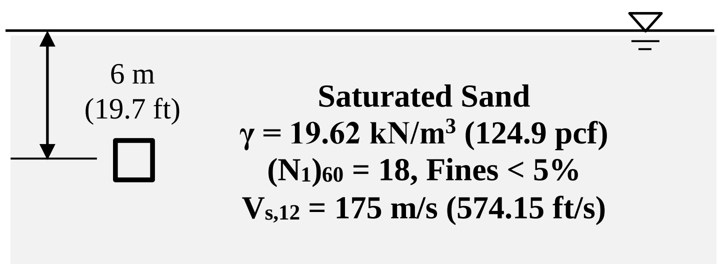

Figure 2.2. Reference soil profile used to develop liquefaction loading maps in the proposed simplified uniform hazard liquefaction procedure

Figure 2.3. Liquefaction loading map (T_R = 1,033 years) showing contours of $CSR^{ref}(\%)$ for a portion of the Salt Lake Valley in Utah.

In interpreting a liquefaction loading map such as the one presented in Figure 2.3, a qualitative assessment of relative liquefaction hazard across a geographic area at the targeted return period can be made. Higher values of $CSR^{ref}(\%)$ imply higher levels of seismic loading for liquefaction triggering. Soils located in areas of higher $CSR^{ref}(\%)$ will need greater SPT resistance to prevent liquefaction triggering than soils located in areas of lower $CSR^{ref}(\%)$. However, a liquefaction loading map by itself tells the engineer nothing regarding the actual liquefaction hazard at a site because the map does not account for site-specific soil conditions. A procedure will subsequently be derived and presented to correct the mapped liquefaction loading values to site-specific liquefaction loading values, which can be used to compute site-specific performance-based estimates of liquefaction triggering hazard at a targeted return period.

A liquefaction loading map should not be confused with a liquefaction hazard map, which attempts to account for actual soil conditions at each mapped location. The difficulty in obtaining site-specific subsurface data for all locations across a geologic region is significant, indeed. Furthermore, liquefaction hazard maps tell the engineer nothing regarding the liquefaction triggering hazard with depth in the actual soils at the site. Thus, liquefaction hazard maps constitute a preliminary hazard assessment and planning tool, and can be very helpful to engineers if used properly. However, liquefaction hazard map results should be interpreted with caution and an understanding that local site conditions and actual liquefaction hazard may deviate significantly from what is mapped.

2.3.1.1 Site-Specific Correction for CSR^{ref}

Because CSR^{ref} was developed using the reference soil profile, it must be corrected for site-specific soil conditions and depths to be used in computing site-specific uniform hazard values of FS_L, P_L, and N_{req}. If CSR^{site} represents the site-specific uniform hazard value of *CSR*, then CSR^{ref} and CSR^{site} can be related as:

$$\ln\left(CSR^{site}\right) = \ln\left(CSR^{ref}\right) + \Delta CSR \tag{14}$$

where ΔCSR is a site-specific correction factor. Rearranging Equation (14), we can solve for ΔCSR as:

$$\Delta CSR = \ln\left(CSR^{site}\right) - \ln\left(CSR^{ref}\right) = \ln\left(\frac{CSR^{site}}{CSR^{ref}}\right) \tag{15}$$

Similar to Equation (8), the magnitude- and stress-corrected *CSR* for level or near-level ground according to Boulanger and Idriss (2012) is computed as:

$$CSR_{M=7.5,\sigma_v'=1atm} = 0.65\frac{\sigma_v}{\sigma_v'}\frac{a_{\max}}{g}r_d\frac{1}{MSF}\frac{1}{K_\sigma} = 0.65\frac{\sigma_v}{\sigma_v'}\frac{\left(F_{pga}\cdot PGA_{rock}\right)}{g}r_d\frac{1}{MSF}\frac{1}{K_\sigma} \tag{16}$$

where F_{pga} is the soil amplification factor corresponding to the peak ground acceleration (PGA), and PGA_{rock} is the PGA corresponding to bedrock (i.e. V_s=760 m/s). Equations for r_d, MSF, and K_σ as defined in Idriss and Boulanger (2008, 2010) are provided in later sections of this report. If Equation (16) is substituted into Equation (15), then Equation (15) can be rewritten as:

$$\Delta CSR = \ln\left[\frac{0.65\left(\dfrac{\sigma_v}{\sigma_v'}\right)^{site}\left(\dfrac{F_{pga}^{site}\cdot PGA_{rock}^{site}}{g}\right)\cdot r_d^{site}\cdot\left(\dfrac{1}{MSF^{site}}\right)\cdot\left(\dfrac{1}{K_\sigma^{site}}\right)}{0.65\left(\dfrac{\sigma_v}{\sigma_v'}\right)^{ref}\left(\dfrac{F_{pga}^{ref}\cdot PGA_{rock}^{ref}}{g}\right)\cdot r_d^{ref}\cdot\left(\dfrac{1}{MSF^{ref}}\right)\cdot\left(\dfrac{1}{K_\sigma^{ref}}\right)}\right] \tag{17}$$

Because there should be no difference in the ground motions between the reference soil profile and the actual soil profile, $PGA_{rock}^{site} = PGA_{rock}^{ref}$. Therefore, Equation (17) can be simplified as:

$$\begin{aligned}\Delta CSR &= \ln\left(\frac{\left(\sigma_v/\sigma_v'\right)^{site}}{\left(\sigma_v/\sigma_v'\right)^{ref}}\right)+\ln\left(\frac{F_{pga}^{site}}{F_{pga}^{ref}}\right)+\ln\left(\frac{r_d^{site}}{r_d^{ref}}\right)-\ln\left(\frac{MSF^{site}}{MSF^{ref}}\right)-\ln\left(\frac{K_\sigma^{site}}{K_\sigma^{ref}}\right)\\ &= \Delta CSR_\sigma+\Delta CSR_{F_{pga}}+\Delta CSR_{r_d}+\Delta CSR_{MSF}+\Delta CSR_{K_\sigma}\end{aligned} \tag{18}$$

where ΔCSR_σ, ΔCSR_{Fpga}, ΔCSR_{rd}, ΔCSR_{MSF}, and $\Delta CSR_{K\sigma}$ are site-specific correction factors for stress, soil amplification, shear stress reduction, earthquake magnitude, and overburden pressure, respectively.

2.3.1.2 Correction for Vertical Stress, ΔCSR_σ

The relationship for the stress correction factor, ΔCSR_σ is defined as:

$$\Delta CSR_\sigma = \ln\left[\frac{\left(\sigma_v/\sigma_v'\right)^{site}}{\left(\sigma_v/\sigma_v'\right)^{ref}}\right] \tag{19}$$

If the liquefaction parameter map for CSR^{ref} (%) was developed using the reference soil profile shown in Figure 2.2, then Equation (19) can be simplified as:

$$\Delta CSR_{\sigma} = \ln\left[\frac{\left(\sigma_v / \sigma_v'\right)^{site}}{2}\right] \tag{20}$$

Mayfield et al. (2010) used weight-volume relationships to investigate the possibility of simplifying the stress correction factor in their simplified procedure. By substituting specific gravity and void ratio for the vertical stress terms, and then by assuming that the site-specific void ratio and specific gravity were the same as those used in the reference soil profile, Mayfield et al. developed a simplified equation for their stress correction factor that was simply a function of depth and depth to groundwater. Mayfield et al. demonstrated that this simplified equation was quite insensitive to changes in void ratio, and thus introduced relatively little error into their computed results. A similar investigation was performed with ΔCSR_{σ} in this study to evaluate the possibility of developing a simplified relationship for Equation (20). However, we found that a simplified equation after the manner demonstrated by Mayfield et al. introduces significant error into the computed results of our proposed simplified liquefaction procedure, likely due to the fact that our proposed procedure is based on a natural logarithm function (i.e. Equation (15)), whereas the Mayfield et al. (2010) simplified procedure is based on a linear relationship.

2.3.1.3 Correction for Soil Amplification, ΔCSR_{Fpga}

The relationship for the soil amplification factor, ΔCSR_{Fpga} is defined as:

$$\Delta CSR_{F_{pga}} = \ln\left(\frac{F_{pga}^{site}}{F_{pga}^{ref}}\right) \tag{21}$$

If the value of F_{pga}^{ref} for the reference soil profile is fixed at 1, then the correction factor for soil amplification can be written as:

$$\Delta CSR_{F_{pga}} = \ln\left(\frac{F_{pga}^{site}}{1}\right) = \ln\left(F_{pga}^{site}\right) \tag{22}$$

Thus the only parameter required to calculate the soil amplification factor is the F_{pga}^{site} value from AASHTO 2012 Table 3.10.3.2-1 corresponding to the site of interest. This table is included here as a reference (Table 2.1). The *PGA* value used to determine F_{pga}^{site} from the table should be calculated from the USGS 2008 (USGS 1996 for Alaska) interactive deaggregation website for the return period of interest (e.g., 2% probability of exceedance in 21 years, T_R = 1039).

Table 2.1. Values of Site Factor, F_{pga}, at Zero-Period on Acceleration Spectrum (from AASHTO 2012 Table 3.10.3.2-1)

Site Class	Peak Ground Acceleration Coefficient (*PGA*)[1]				
	PGA < 0.10	*PGA* = 0.20	*PGA* = 0.30	*PGA* = 0.40	*PGA* > 0.50
A	0.8	0.8	0.8	0.8	0.8
B	1.0	1.0	1.0	1.0	1.0
C	1.2	1.2	1.1	1.0	1.0
D	1.6	1.4	1.2	1.1	1.0
E	2.5	1.7	1.2	0.9	0.9
F[2]	*	*	*	*	*

Notes:

[1]Use straight-line interpolation for intermediate values of *PGA*.

[2]Site-specific geotechnical investigation and dynamic site response analysis should be performed for all sites in Site Class F.

If an engineer prefers to use an empirical model for soil amplification, such as the Stewart et al. (2003) model, the ΔCSR_{Fpga} term can be adjusted for the desired model. For example, in the Stewart et al. (2003) model, the median amplification factor F_{pga} is defined as:

$$F_{pga} = \exp\left[a + b\ln\left(PGA_{rock}\right)\right] \tag{23}$$

where PGA_{rock} is in units of g, *a* and *b* are regression coefficients defined by Stewart et al. (2003). Using Equation (23), the correction for the soil amplification factor can be written as:

$$\Delta CSR_{F_{pga}} = \ln\left(\frac{F_{pga}^{site}}{F_{pga}^{ref}}\right) = \ln\left(\frac{\exp\left(a^{site} + b^{site}\ln\left(PGA_{rock}^{site}\right)\right)}{\exp\left(a^{ref} + b^{ref}\ln\left(PGA_{rock}^{ref}\right)\right)}\right)$$

$$= \left(a^{site} + b^{site}\ln\left(PGA_{rock}^{site}\right)\right) - \left(a^{ref} + b^{ref}\ln\left(PGA_{rock}^{ref}\right)\right) \tag{24}$$

There should be no difference between PGA_{rock}^{site} and PGA_{rock}^{ref}, so Equation (24) can be simplified to:

$$\Delta CSR_{F_{pga}} = \left(a^{site} - a^{ref}\right) + \ln\left(PGA_{rock}\right)\left(b^{site} - b^{ref}\right) \tag{25}$$

If the liquefaction parameter map for CSR^{ref} (%) was developed using the reference soil profile shown in Figure 2.2, then a^{ref} = - 0.15, b^{ref} = - 0.13 (see Stewart et al., 2003), and Equation (25) would become:

$$\Delta CSR_{F_{pga}} = \left(a^{site} + 0.15\right) + \ln\left(PGA_{rock}^{site}\right)\left(b^{site} + 0.13\right) \tag{26}$$

2.3.1.4 Correction for Shear Stress Reduction, ΔCSR_{rd}

The shear stress reduction factor, r_d, was defined by Boulanger and Idriss (2012, 2014) as:

$$r_d = \exp\left[\alpha + \beta \cdot M_w\right] \tag{27}$$

$$\alpha = -1.012 - 1.126\sin\left(\frac{z}{11.73} + 5.133\right) \tag{28}$$

$$\beta = 0.106 + 0.118\sin\left(\frac{z}{11.28} + 5.142\right) \tag{29}$$

where z represents sample depth in meters and M_w is the mean moment magnitude. Thus the equation for ΔCSR_{rd} becomes:

$$\Delta CSR_{r_d} = \ln\left(\frac{r_d^{site}}{r_d^{ref}}\right) = \ln\left(\frac{\exp\left(\alpha^{site} + \beta^{site} \cdot \mathrm{M}_w^{site}\right)}{\exp\left(\alpha^{ref} + \beta^{ref} \cdot \mathrm{M}_w^{ref}\right)}\right) \tag{30}$$

Both the site soil profile and the reference soil profile experience the same ground motions, so $M_w^{site} = M_w^{ref}$. Therefore, Equation (30) can be written as:

$$\Delta CSR_{r_d} = \left(\alpha^{site} - \alpha^{ref}\right) + M_w^{site}\left(\beta^{site} - \beta^{ref}\right) \tag{31}$$

Mayfield et al. (2010) demonstrated that the r_d term in the Cetin et al. (2004) model is relatively insensitive to the value of M_w for a particular range (M_w = 5.97 to 7.70). This observation allowed the correction factor for r_d to use a standard M_w value of 6.5 for all analyses. In this study, the r_d value from the Boulanger and Idriss (2014) model was found to be quite sensitive to M_w. This sensitivity is clear in Figure 2.4, which illustrates the variability of r_d with depth and M_w (5.5 to 8.0). Due to the significant discrepancy between r_d values for different M_w, the simplified Boulanger and Idriss (2014) method requires M_w^{site} to remain in Equation (31). For the reference soil profile used in this study (Figure 2.2), α^{ref} = -0.3408 and β^{ref} = 0.0385. Thus Equation (31) becomes:

$$\Delta CSR_{r_d} = \left(\alpha^{site} + 0.341\right) + M_w^{site}\left(\beta^{site} - 0.0385\right) \tag{32}$$

Equation (32) can also be written in terms of depth to the site-specific soil layer (in meters) from the ground surface, z^{site} as:

$$\begin{aligned}\Delta CSR_{r_d} = &\left(-0.6712 - 1.126\sin\left(\frac{z^{site}}{11.73} + 5.133\right)\right) \\ &+ M_w^{site}\left(0.0675 + 0.118\sin\left(\frac{z^{site}}{11.28} + 5.142\right)\right)\end{aligned} \tag{33}$$

where the value of M_w^{site} is the <u>mean</u> moment magnitude from the 2008 (1996 for Alaska) USGS interactive deaggregation website for the return period of interest (e.g., 2% probability of exceedance in 21 years, T_R = 1039). The value of ΔCSR_{rd} varies with depth, and therefore must be calculated for each layer in the site-specific soil profile.

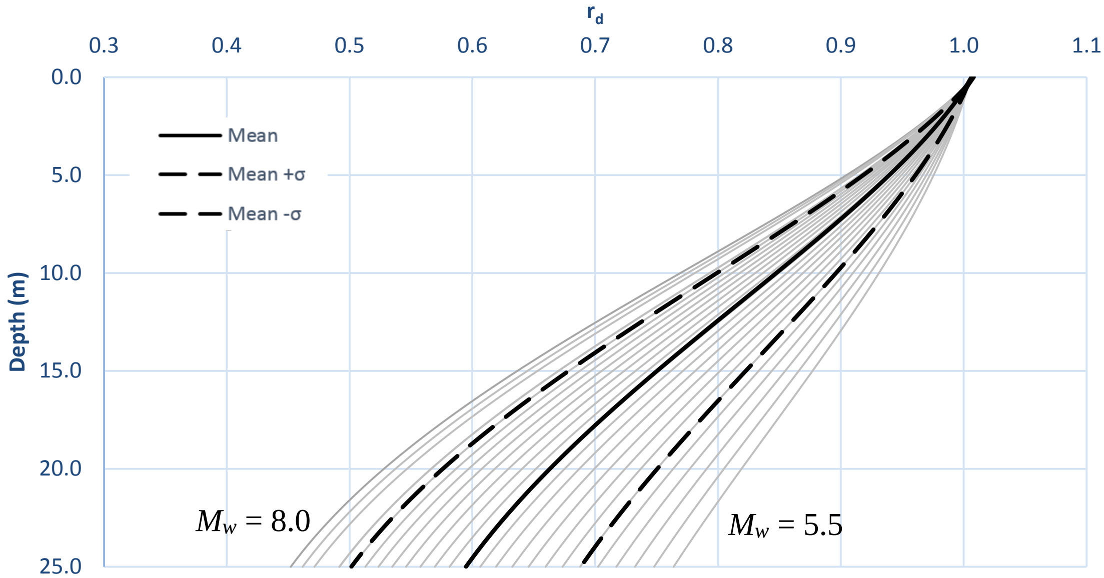

Figure 2.4. Shear stress reduction factor (r_d) vs. depth for a range of M_w values (5.5 to 8.0) according to the Boulanger and Idriss (2014) model.

2.3.1.5 Correction for Magnitude Scaling Factor, ΔCSR_{MSF}

If the *MSF* as calculated in the Idriss and Boulanger (2010, 2012) model is to be used, then there should be no difference in the earthquake magnitude between the reference soil profile and the actual soil profile. In this case, $MSF^{site} = MSF^{ref}$ which indicates that $\Delta CSR_{MSF} = 0$ and therefore ΔCSR_{MSF} can be excluded from Equation (18).

If the *MSF* as calculated in the updated Boulanger and Idriss (2014) model is to be used, then $MSF = f\left(N_{1,60,cs}\right)$. Because MSF is a function of $N_{1,60,cs}$, it is possible that $MSF^{site} \neq MSF^{ref}$ because it is likely that $\left(N_1\right)_{60,cs}$ varies with depth in the actual soil profile. Thus ΔCSR_{MSF} must be included in Equation (18). Using the equation for *MSF* from the updated Boulanger and Idriss (2014) model, this correction factor can be written as:

$$\Delta CSR_{MSF} = -\ln\left(\frac{MSF^{site}}{MSF^{ref}}\right) = -\ln\left(\frac{1+\left(MSF_{\max}^{site}-1\right)\left(8.64\exp\left(\frac{-M_w^{site}}{4}\right)-1.325\right)}{1+\left(MSF_{\max}^{ref}-1\right)\left(8.64\exp\left(\frac{-M_w^{ref}}{4}\right)-1.325\right)}\right) \tag{34}$$

$$MSF_{\max} = 1.09 + \left(\frac{\left(N_1\right)_{60,cs}}{31.5}\right)^2 \leq 2.2 \tag{35}$$

where $\left(N_1\right)_{60,cs}$ represents the clean sand-equivalent SPT resistance value corrected to 60% efficiency and 1 atm overburden pressure as computed using the equations provided by Idriss and Boulanger (2008, 2010). Note that there is no difference in the magnitude of the ground motions between the reference map and the site. Thus, M_w^{ref} can be replaced with M_w^{site}. Therefore, if the liquefaction parameter map for CSR^{ref} (%) was developed using the reference soil profile shown in Figure 2.2, then $MSF_{\max}^{ref}$ = 1.417 and Equation (34) can be written as:

$$\Delta CSR_{MSF} = -\ln\left[\frac{1+\left(MIN\begin{cases}\left(\frac{\left(N_1\right)_{60,cs}^{site}}{31.5}\right)^2+0.09\\ 1.2\end{cases}\right)\cdot\left(8.64\exp\left(\frac{-M_w^{site}}{4}\right)-1.325\right)}{3.603\exp\left(\frac{-M_w^{site}}{4}\right)+0.447}\right] \tag{36}$$

The value of ΔCSR_{MSF} must be calculated for each layer in the soil profile because $MSF_{\max}^{site}$ is a function of $\left(N_1\right)_{60,cs}$, which likely varies throughout the soil profile. The value of M_w^{site} is the mean moment magnitude from the 2008 (1996 for Alaska) USGS interactive deaggregation website for the return period of interest (e.g., 2% probability of exceedance in 21 years, T_R = 1039). This should be the same value as M_w^{site} used to calculate the ΔCSR_{rd} term in Equation (33).

2.3.1.6 Correction for Overburden Pressure, ΔCSR$_{K\sigma}$

Both the 2010 and 2014 versions of the Boulanger and Idriss model use the same overburden correction factor, K_σ:

$$K_\sigma = 1 - C_\sigma \ln\left(\frac{\sigma'_v}{P_a}\right) \leq 1.1 \tag{37}$$

$$C_\sigma = \frac{1}{18.9 - 2.55\sqrt{(N_1)_{60,cs}}} \leq 0.3 \tag{38}$$

where P_a is 1 atmosphere of pressure (i.e. 1 atm, 101.3 kPa, 0.2116 psf). Note that the value $(N_1)_{60,cs}$ must be computed using the equations found in Idriss and Boulanger (2008, 2010). Idriss and Boulanger (2010) commented that the K_σ limit of 1.1 has a somewhat negligible effect. Therefore, the simplified method derived here will not use the restriction on K_σ. However, the limit of 0.3 for values of C_σ will be incorporated. Now the correction term $\Delta CSR_{K\sigma}$ can be written as:

$$\Delta CSR_{K_\sigma} = -\ln\left(\frac{K_\sigma^{site}}{K_\sigma^{ref}}\right) = -\ln\left(\frac{1 - C_\sigma^{site}\ln\left(\frac{(\sigma'_v)^{site}}{P_a}\right)}{1 - C_\sigma^{ref}\ln\left(\frac{(\sigma'_v)^{ref}}{P_a}\right)}\right) \tag{39}$$

If the liquefaction parameter map for CSR^{ref} (%) was developed using the reference soil profile shown in Figure 2.2, then $C_\sigma^{ref} = 0.147$, $K_\sigma^{ref} = 1.0682$, and Equation (39) would become:

$$\Delta CSR_{K_\sigma} = -\ln\left(\frac{1 - \left(MIN\left\{\begin{matrix}0.3 \\ \dfrac{1}{18.9 - 2.55\sqrt{(N_1)_{60,cs}^{site}}}\end{matrix}\right.\right) \cdot \ln\left(\frac{(\sigma'_v)^{site}}{P_a}\right)}{1.0682}\right) \tag{40}$$

Note that if $(N_1)_{60,cs}$ is restricted to ≤ 37 then the coefficient C_σ as defined in Equation (38) will remain below its maximum value of 0.3.

2.3.1.7 Equations for CSR^{site}, N_{req}^{site}, FS_L, and P_L

Once the $CSR^{ref}\,(\%)$ is obtained from the appropriate (i.e. hazard-targeted) map and the appropriate correction factors are computed using Equations (20), (22), (33), (36) (neglected if using Idriss and Boulanger 2008 *MSF* instead of the updated Boulanger and Idriss 2014 *MSF*) and (40), the site-specific hazard-targeted CSR^{site} can be computed for site-specific soil layer *i* using the following equation (from Equation (14)):

$$\left(CSR^{site}\right)_i = \exp\left[\ln\left(\frac{CSR^{ref}\,(\%)}{100}\right) + \left(\Delta CSR_{\sigma}\right)_i + \left(\Delta CSR_{F_{pga}}\right)_i + \left(\Delta CSR_{r_d}\right)_i + \left(\Delta CSR_{MSF}\right)_i + \left(\Delta CSR_{K_\sigma}\right)_i\right] \quad (41)$$

This $\left(CSR^{site}\right)$ value can then be used to calculate N_{req}^{site}, FS_L, or P_L for site-specific soil layer *i*. To calculate the value of $\left(N_{req}^{site}\right)_i$, solve the following polynomial iteratively (from Equation (13)):

$$0 = \left(\frac{\left(N_{req}^{site}\right)_i}{14.1}\right) + \left(\frac{\left(N_{req}^{site}\right)_i}{126}\right)^2 - \left(\frac{\left(N_{req}^{site}\right)_i}{23.6}\right)^3 + \left(\frac{\left(N_{req}^{site}\right)_i}{25.4}\right)^4 - 2.67 - \ln\left(\left(CSR^{site}\right)_i\right) \quad (42)$$

Alternatively, the following closed-form regression equation will provide a very close approximation of N_{req}^{site} given CSR^{site} (R^2=0.999):

$$\begin{aligned}\left(N_{req}^{site}\right)_i = {} & 1.237\cdot\left(\ln\left(\frac{1}{\left(CSR^{site}\right)_i}\right)\right)^4 - 4.9183\cdot\left(\ln\left(\frac{1}{\left(CSR^{site}\right)_i}\right)\right)^3 \\ & + 1.7624\cdot\left(\ln\left(\frac{1}{\left(CSR^{site}\right)_i}\right)\right)^2 - 5.4733\cdot\left(\ln\left(\frac{1}{\left(CSR^{site}\right)_i}\right)\right) + 33.65\end{aligned} \quad (43)$$

Equation (43) is valid for $0.08 \le \left(CSR^{site}\right)_i \le 1.26$. Outside of these bounds, the polynomial should be solved iteratively.

To solve for the uniform-hazard FS_L for the soil layer i, use Equation (13) as:

$$\left(FS_L\right)_i = \frac{\left(CRR^{site}\right)_i}{\left(CSR^{site}\right)_i} = \frac{\exp\left[\left(\frac{\left(\left(N_1\right)_{60,cs}\right)_i}{14.1}\right) + \left(\frac{\left(\left(N_1\right)_{60,cs}\right)_i}{126}\right)^2 - \left(\frac{\left(\left(N_1\right)_{60,cs}\right)_i}{23.6}\right)^3 + \left(\frac{\left(\left(N_1\right)_{60,cs}\right)_i}{25.4}\right)^4 - 2.67\right]}{\left(CSR^{site}\right)_i} \tag{44}$$

To solve for the uniform hazard P_L for the soil layer i, use the following relationship:

$$\left(P_L\right)_i = \Phi\left[-\frac{\ln\left(\frac{\left(CRR^{site}\right)_i}{\left(CSR^{site}\right)_i}\right)}{\sigma_\varepsilon}\right] = \Phi\left[-\frac{\ln\left(\left(FS_L\right)_i\right)}{\sigma_\varepsilon}\right] \tag{45}$$

Where σ_ε is 0.13 if parametric uncertainty (i.e., uncertainty in measuring $\left(N_1\right)_{60,cs}$ and estimating seismic loading) is neglected, and σ_ε is 0.277 if parametric uncertainty is considered. Because it is impossible to completely eliminate uncertainty when measuring parameters such as $\left(N_1\right)_{60,cs}$ in the field, it is recommended that $\sigma_\varepsilon = 0.277$.

2.4 Empirical Lateral Spread Displacement Model

The simplified lateral spread displacement model is derived from the widely-used empirical lateral spread model originally presented by Bartlett and Youd (1995). Their model was regressed from a large database of lateral spread case histories from Japan and the western United States, and a large number of parameters related to soil properties, slope geometry, and level of ground motion were statistically evaluated. Bartlett and Youd identified the parameters that produced the best regression, and from those parameters regressed their original empirical predictive relationship. Youd et al. (2002) later updated their original empirical model by using an expanded and corrected version of the 1995 database. The updated Bartlett and Youd empirical model has since been adopted as the state of practice in much of the world, and it is routinely applied on a wide variety of projects in all types of seismic environments. The Youd et al. (2002) updated empirical model is given as:

$$\overline{\log D_H} = b_0 + b_1 M + b_2 \log R^* + b_3 R + b_4 \log W + b_5 \log S + b_6 \log T_{15} + b_7 \log\left(100 - F_{15}\right) + b_8 \log\left(D50_{15} + 0.1\right) \quad (46)$$

where

D_H = median computed permanent lateral spread displacement (m)
M = earthquake moment magnitude
R = the closest horizontal distance from the site to the source (km)
W = the free-face ratio (%)
S = the ground slope (%)
T_{15} = the cumulative thickness (in upper 20 m) of all saturated soil layers with corrected Standard Penetration Test (SPT) blowcounts (i.e., $(N_1)_{60}$) less than 15 blows/foot (m)
F_{15} = the average fines content of the soil comprising T_{15} (%)
$D50_{15}$ = the average mean grain size of the soil comprising T_{15} (mm)

and R* is computed as

$$R^* = R + 10^{0.89M - 5.64} \quad (47)$$

Model coefficients b_0 through b_8 are given in Table 2.2.

Table 2.2 Regression coefficients for the Youd et al. (2002) empirical lateral spread model

Model	b_0	b_1	b_2	b_3	b_4	b_5	b_6	b_7	b_8
Ground slope	-16.213	1.532	-1.406	-0.012	0	0.338	0.540	3.413	-0.795
Free Face	-16.713	1.532	-1.406	-0.012	0.592	0	0.540	3.413	-0.795

2.4.1 Full Performance-based Lateral Spread Model

Kramer et al. (2007) suggested that performance-based estimates of lateral spread displacement could be computed by modifying an empirical lateral spreading model in such a way so as to insert it directly into a probabilistic seismic hazard analysis (PSHA). Such a modification could be performed by separating the model terms associated with seismic loading (i.e. the Loading Parameter, $\mathscr{L}$) from the model terms associated with local site and geometry conditions (i.e. the Site Parameter, $\mathscr{S}$). Therefore, a modified form of any given empirical lateral spread model could be written as:

$$\mathscr{D} = \mathscr{L} - \mathscr{S} + \varepsilon \tag{48}$$

where $\mathscr{D}$ is the transformed (e.g. log, ln, square root) lateral spread displacement, and $\mathscr{L}$, $\mathscr{S}$, and ε represent the apparent loading, site, and uncertainty terms.

Following the Kramer et al. (2007) framework, Franke and Kramer (2014) demonstrated how the Youd et al. (2002) empirical model for lateral spread displacement could be adapted to develop fully probabilistic estimates of lateral spread displacement. The performance-based form of the Youd et al. (2002) was shown to be:

$$\log D_H = \mathscr{L} - \mathscr{S} + \varepsilon \tag{49}$$

where

$$\mathscr{L} = b_1 M + b_2 \log R^* + b_3 R \tag{50}$$

$$\mathscr{S} = -\left(b_0 + b_4 \log W + b_5 \log S + b_6 \log T_{15} + b_7 \log\left(100 - F_{15}\right) + b_8 \log\left(D50_{15} + 0.1\right)\right) \tag{51}$$

$$\varepsilon = \sigma_{\log D_H} \Phi^{-1}\left[P\right] \tag{52}$$

$$\sigma_{\log D_H} = 0.197 \tag{53}$$

If computing the probability of exceeding some given displacement, d, Equation (53) can be incorporated as:

$$P\left[D_H > d\right] = 1 - \Phi\left[\frac{\log d - \overline{\log D_H}}{\sigma_{\log D_H}}\right] = 1 - \Phi\left[\frac{\log d - \overline{\log D_H}}{0.197}\right] \tag{54}$$

Because a given site should produce a single value of $\mathscr{S}$ to be used in design, the left side of Equation (49) can be thought of as a simple linear function of $\mathscr{L}$ with a constant y-intercept equal to $\mathscr{S}$ and a data spread characterized by ε, as shown in Figure 2.5. Because $\mathscr{S}$ is considered a constant value in the performance-based analysis, multiple lateral spread hazard curves could be developed for a site for different values of $\mathscr{S}$ (Figure 2.6). Thus, the effect of varying site and/or geometry conditions when computing probabilistic lateral spread displacements could be evaluated.

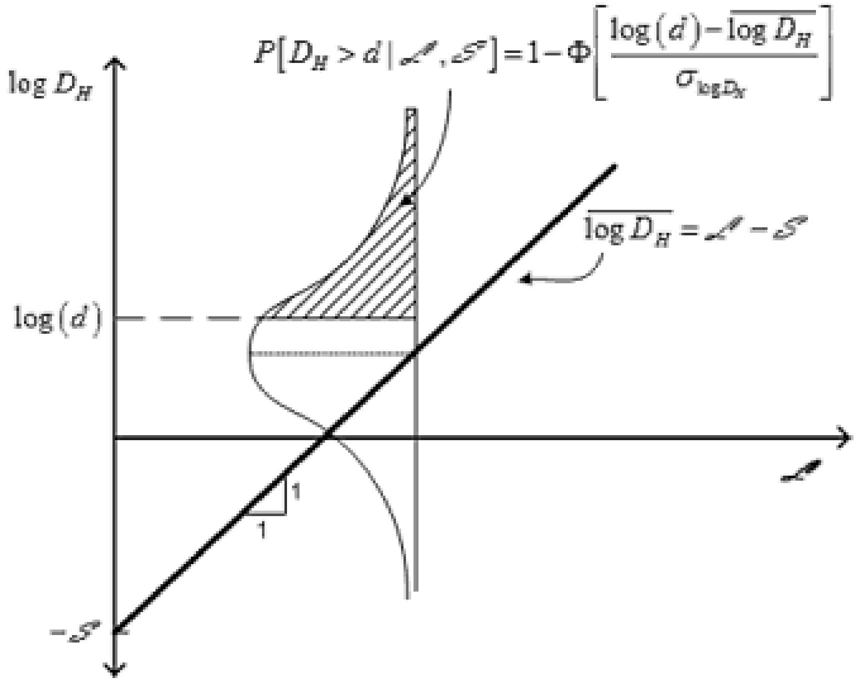

Figure 2.5 Schematic diagram of the fully probabilistic lateral spread model with Youd et al. (2002) (after Franke and Kramer 2013)

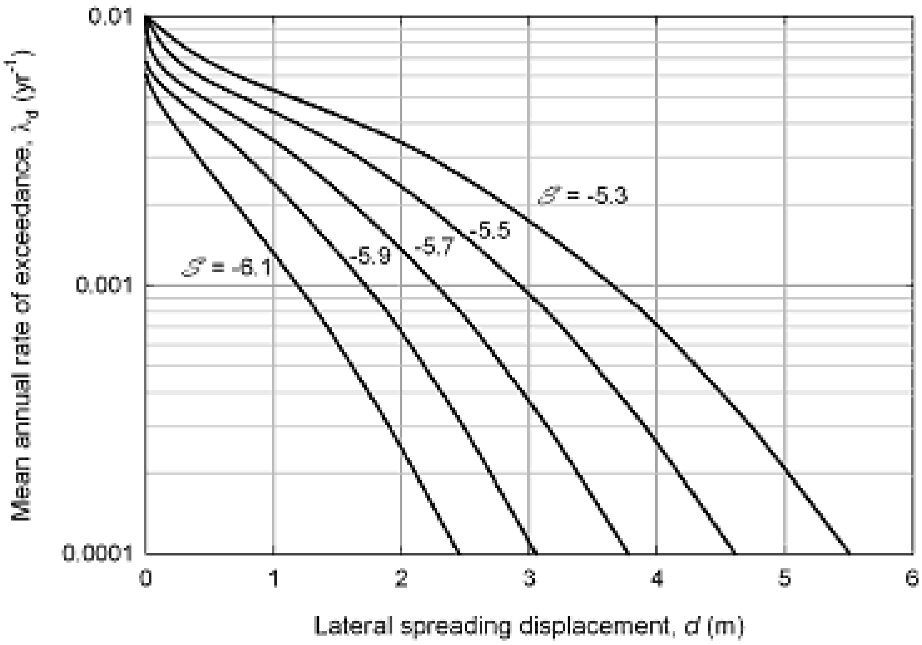

Figure 2.6 Variations of lateral spread hazard curves as a function of the site term, $\mathscr{S}$ (after Kramer et al. 2007)

Though it is not an actual or measurable ground motion parameter, the apparent loading parameter in Equation (50) is a function of magnitude and distance and attenuates in a manner similar to measurable ground motion intensity measures described by traditional Ground Motion Prediction Equations (GMPEs). In the context of the Youd et al. (2002) model, the apparent loading term, therefore, acts in a manner analogous to an Intensity Measure (*IM)*, the variation of whose median value with *M* and *R* is described by Equation (50).

By incorporating Equations (50) and (51) into the probabilistic framework presented in Equation (54) and assigning all of the uncertainty in the Youd et al. (2002) model to the conditional displacement calculation, a performance-based model can be expressed in terms of lateral spread displacement conditional upon the site parameter as:

$$\lambda_{D_H|\mathscr{S}}(d \mid \mathscr{S}) = \sum_{i=1}^{N_{\mathscr{L}}} P\left[D_H > d \mid \mathscr{S}, \mathscr{L}_i\right] \Delta\lambda_{\mathscr{L}_i} \tag{55}$$

where $\lambda_{D_H|\mathscr{S}}(d \mid \mathscr{S})$ is the mean annual rate of exceeding a displacement d conditional upon site conditions S, $N_{\mathscr{L}}$ is the number of loading parameter increments required to span the range of possible $\mathscr{L}$ values, and $\Delta\lambda_{\mathscr{L}_i}$ is the increment of the apparent loading parameter in hazard space. For a single source, Equation (55) can also be written as:

$$\lambda_{D_H|\mathscr{S}}\left(d\,|\,\mathscr{S}\right)=\nu\sum_{i=1}^{N_{\mathscr{L}}}P\left[D_H>d\,|\,\mathscr{S},\mathscr{L}_i\right]P\left[\mathscr{L}_i\right] \tag{56}$$

where ν is the mean annual rate of exceeding a minimum magnitude of interest for a given seismic source. Because the loading parameter is a function of magnitude and distance (which are commonly assumed to be independent in PSHA work) and can be affected by multiple seismic sources, Equation (56) can be rewritten as:

$$\lambda_{D_H|\mathscr{S}}\left(d\,|\,\mathscr{S}\right)=\sum_{i=1}^{N_S}\nu_i\sum_{j=1}^{N_M}\sum_{k=1}^{N_R}P\left[D_H>d\,|\,\mathscr{S},M=m_j,R=r_k\right]P\left[M=m_j,R=r_k\right] \tag{12}$$

which is very similar to the PSHA framework commonly used to compute uniform hazard estimates of ground motions. Therefore, Equations (49) through (54) can be incorporated into common seismic hazard analysis software such as EZ-FRISK or OpenSHA to develop uniform hazard estimates of lateral spread displacement and displacement hazard curves.

2.4.2 Simplified Performance-based Lateral Spread Model

If a generic reference site is used to compute $\mathscr{S}$, then a series of performance-based lateral spread analyses could be performed across a grid to develop contour maps of lateral spread displacement corresponding to various return periods of interest. These maps are called lateral spread reference maps. For example, a reference site for the derivation of the simplified performance-based lateral spread procedure is presented in Figure 2.7. This profile was chosen based on the profile used to develop the full performance-based method to be consistent. Values of 3.0m, 20%, and 0.2mm are computed for the lateral spread parameters T_{15}, F_{15}, and $D50_{15}$, respectively. As shown in Figure 2.7, the geometry of the site constitutes a ground slope condition with ground slope (i.e. S) equal to 1%. The resulting value of $\mathscr{S}$ for the reference site, as computed from Equation (51), is therefore equal to 9.043.

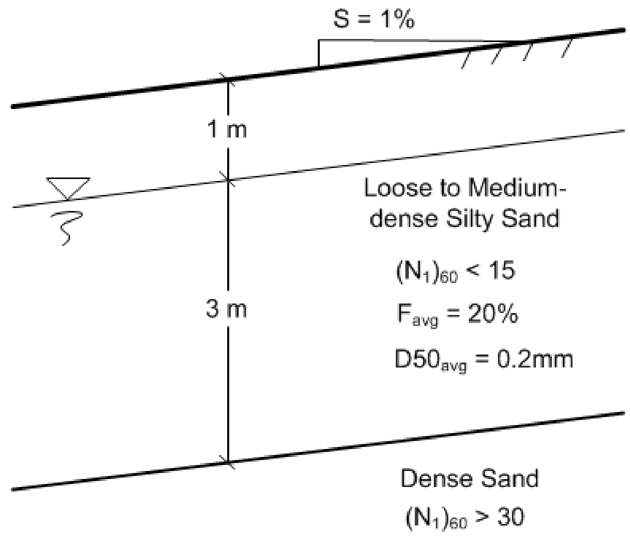

Figure 2.7 Reference soil profile used to derive the simplified performance-based lateral spread approximation

The lateral spread displacement corresponding to the generic reference site could therefore be obtained from the appropriate map and adjusted in order to provide site-specific lateral spread displacements corresponding to the desired return period. The equation for this site-specific adjustment is given as:

$$\left[\log D_H\right]^{site} = \left[\log D_H\right]^{ref} + \Delta D_H \tag{57}$$

where $\left[\log D_H\right]^{site}$ is the logarithm of the lateral spread displacement adjusted for site-specific conditions, $\left[\log D_H\right]^{ref}$ is the logarithm of the lateral spread displacement corresponding to the reference site (obtained from the map), and ΔD_H is the adjustment factor computed by the engineer. By substituting Equation (49) into Equation (57), the adjustment factor can be written as:

$$\Delta D_H = \left(\mathscr{L} - \mathscr{S}\right)^{site} - \left(\mathscr{L} - \mathscr{S}\right)^{ref} = \left(\mathscr{L}^{site} - \mathscr{L}^{ref}\right) + \left(\mathscr{S}^{ref} - \mathscr{S}^{site}\right) \tag{58}$$

However, because $\mathscr{L}^{site} = \mathscr{L}^{ref}$, Equation (58) can be simplified as:

$$\Delta D_H = \mathscr{S}^{ref} - \mathscr{S}^{site} \tag{59}$$

If Equation (51) is substituted for $\mathcal{S}$, then Equation (59) can be rewritten as:

$$\Delta D_H = -\left[b_0 + b_4 \log W + b_5 \log S + b_6 \log T_{15} + b_7 \log\left(100 - F_{15}\right) + b_8 \log\left(D50_{15} + 0.1\right)\right]^{ref} + \left[b_0 + b_4 \log W + b_5 \log S + b_6 \log T_{15} + b_7 \log\left(100 - F_{15}\right) + b_8 \log\left(D50_{15} + 0.1\right)\right]^{site} \quad (60)$$

By simplifying Equation (60) and inserting model coefficients and parameters for the reference site, the adjustment factor can be computed as:

$$\Delta D_H = b_0^{site} + b_4^{site} \log\left(W^{site}\right) + b_5^{site} \log\left(S^{site}\right) + 0.540 \log\left(\frac{T_{15}^{site}}{3}\right) + 3.413 \log\left(\frac{100 - F_{15}^{site}}{80}\right) - 0.795 \log\left(\frac{D50_{15}^{site} + 0.1}{0.3}\right) + 16.213 \quad (61)$$

where b_4^{site} and b_5^{site} denote site-specific geometry coefficients dependent on the geometry model (i.e. ground slope or free-face) and are provided in Table 2.3. Parameters with the '*site*' superscript denote site-specific soil and geometry parameters determined from the site-specific soil information provided by the engineer.

Table 2.3 Site-specific geometry coefficients for computing the adjustment factor, ΔD_H

Model	b_0^{site}	b_4^{site}	b_5^{site}
Ground Slope	-16.213	0	0.338
Free Face	-16.713	0.592	0

Once the reference lateral spread displacement is obtained from the appropriate (i.e. hazard-targeted) map and the adjustment factor is computed using Equation (61) and Table 2.3, the site-specific hazard-targeted lateral spread displacement (in meters) can be computed as:

$$D_H^{site} = 10^{\left(\left[\log D_H\right]^{ref} + \Delta D_H\right)} \quad (62)$$

2.5 Summary

The derivations of the simplified liquefaction triggering and lateral spread displacement models show how to approximate a full performance-based analysis using simple calculations and mapped reference parameters. The simplified liquefaction triggering procedure is based on the Boulanger and Idriss (2012) probabilistic model while the simplified lateral spread displacement model is based on the Youd et al. (2002) empirical model.

3.0 VALIDATION OF THE SIMPLIFIED MODELS

3.1 Overview

The effectiveness of the simplified methods depends on how closely they approximate the results of a complete site-specific probabilistic seismic hazard analysis. In order to show that the simplified method is as accurate as expected, the simplified and full performance-based methods will be performed for ten sites throughout the United States. These sites will be evaluated for three different return periods: 475, 1033, and 2475 years.

3.1.1 Sites used in the Analysis

The sites chosen for the analysis were selected based on the range of seismicity of each site, as well as their distribution across the United States. Table 3.1 lists the location of these sites as well as their latitudes and longitudes.

Table 3.1 Locations used for the validation of the simplified models

Site	Latitude	Longitude
Butte	46.003	-112.533
Charleston	32.726	-79.931
Eureka	40.802	-124.162
Memphis	35.149	-90.048
Portland	45.523	-122.675
Salt Lake City	40.755	-111.898
San Francisco	37.775	-122.418
San Jose	37.339	-121.893
Santa Monica	34.015	-118.492
Seattle	47.53	-122.3

The tools used to validate the liquefaction triggering model did not allow any sites in Alaska at this point, so the site Anchorage, Alaska (Latitude 61.217, Longitude -149.9) was not used in the validation process for that model. However, the tools used to validate the lateral spread displacement model did have the ability to analyze sites in Alaska so the Anchorage site was used in the validation process for that model.

3.2 Simplified Liquefaction Triggering Model Validation

To calculate the site-specific CSR^{site}, an assumed soil profile was applied at each site. The parameters associated with this soil profile are presented in Figure 3.1.

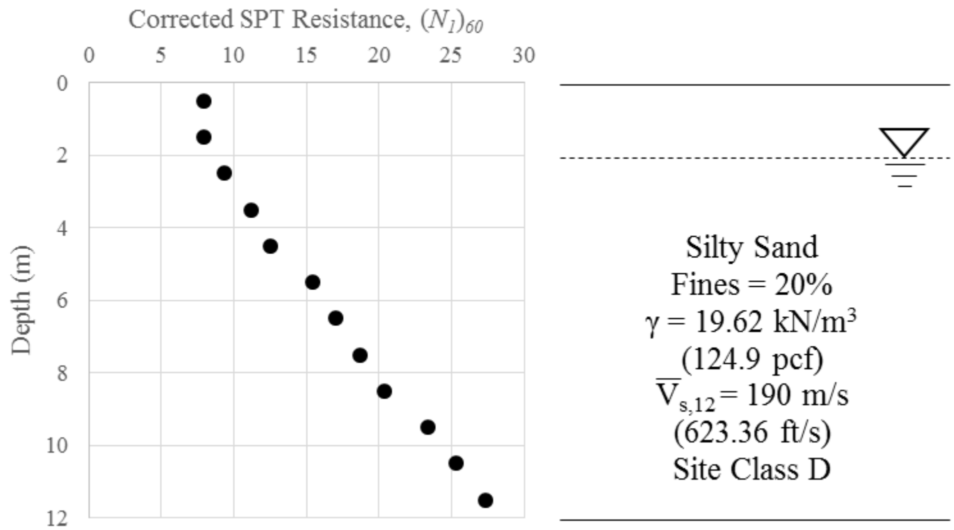

Figure 3.1 Site-specific soil profile used to validate the simplified performance-based model

3.2.1 PBLiquefY

The site-specific analysis for the full performance-based method was performed using PBLiquefY (Franke et al., 2014c). PBLiquefY was also used to create the liquefaction loading maps used to determine the reference value (i.e. CSR^{ref} (%)) necessary for the simplified method. The 2008 USGS ground motion deaggregations were used in both the full and simplified methods.

3.2.2 Validation of the Simplified Performance-Based Cetin et al. (2004) Model

Although the simplified performance-based Cetin et al. (2004) model will not be validated in this report, other publications have verified the use of the simplified Cetin et al. (2004) model (Mayfield et al. 2010; Franke et al 2014d). Mayfield et al. (2010) showed that the computed uniform hazard liquefaction results from the simplified method closely match the liquefaction hazard results from the full performance-based liquefaction analysis at the targeted return period. In future quarterly reports, contour maps of N_{req} from the Cetin et al. (2004) model will be included along with contour maps of CSR^{ref} (%) from the Boulanger and Idriss (2014) model.

3.2.3 Validation of the Simplified Performance-Based Boulanger and Idriss (2012) Model

Using liquefaction loading maps (created using PBLiquefY) and the soil profile selected for the site specific analysis, the value of CSR^{site} was determined for each layer of the site-specific soil profile and for each site using the simplified performance-based method (raw data can be found in the Appendix, Table A.2). These CSR^{site} values were converted to N_{req} values using Equation (42). The resulting N_{req} values are displayed in

Depth conversions for Figure 3.2: 2.5 m (8.20 ft), 3.5 m (11.48 ft), 4.5 m (14.76 ft), 5.5 m (18.04 ft), 6.5 m (21.33 ft), 7.5 m (24.61 ft), 8.5 m (27.89 ft), 9.5 m (31.17 ft), 10.5 m (34.45 ft), 11.5 m (37.73 ft)

Figure 3.2 along with the N_{req} values computed using the full performance-based method. Also included in this plot is N_{site}, which is the in-situ clean sand-equivalent SPT resistance of the site soil profile. Note that both the full performance-based and simplified performance-based methods yield almost identical results for each city represented in this analysis. Overall, the difference between the two methods is within an acceptable amount (within 3.41% on average with a maximum difference of 2.25 blow counts for N_{req}).

The direct comparison of the two methods for three different return periods can be seen in Figure 3.3. Each point on this plot represents a single layer in the site soil profile located in one city for one return period (a total of 300 points). As seen in this plot, the simplified method provides a good approximation of the results from a full probabilistic analysis (R^2 value between 0.996 and 0.997) and provides predictions of N_{req} that account for uncertainty in the model parameters without the need for a full probabilistic analysis. It may seem that the high R^2 values are too good to be true; however, it is important to note that this is a mathematically derived relationship and is expected to be closely correlated with the results of a full probabilistic analysis. If these two values (N_{req} from the simplified method and N_{req} from the full method) were randomly selected samples from a natural population, then these R^2 values would be reason for suspicion.

3.2.3.1Boulanger and Idriss (2014) Updated MSF Term

During the production of this report, a revised Boulanger and Idriss (2014) model was published. This revised model included a new definition of the *MSF* (as explained previously). Though this report discussed the derivation of the simplified performance-based procedure for both the updated Boulanger and Idriss (2014) model and the previous Boulanger and Idriss (2012) model, the software performing the calculations for this mapping study (PBLiquefY) was not able to be updated in time to use the 2014 version of the *MSF* in the validation calculations. Hence, the validation of the simplified Boulanger and Idriss performance-based liquefaction triggering model in this report was performed using the 2012 version of the *MSF*. During the next quarter, the software will be updated to include the option of using the 2014 *MSF* term.

Depth conversions for Figure 3.2: 2.5 m (8.20 ft), 3.5 m (11.48 ft), 4.5 m (14.76 ft), 5.5 m (18.04 ft), 6.5 m (21.33 ft), 7.5 m (24.61 ft), 8.5 m (27.89 ft), 9.5 m (31.17 ft), 10.5 m (34.45 ft), 11.5 m (37.73 ft)

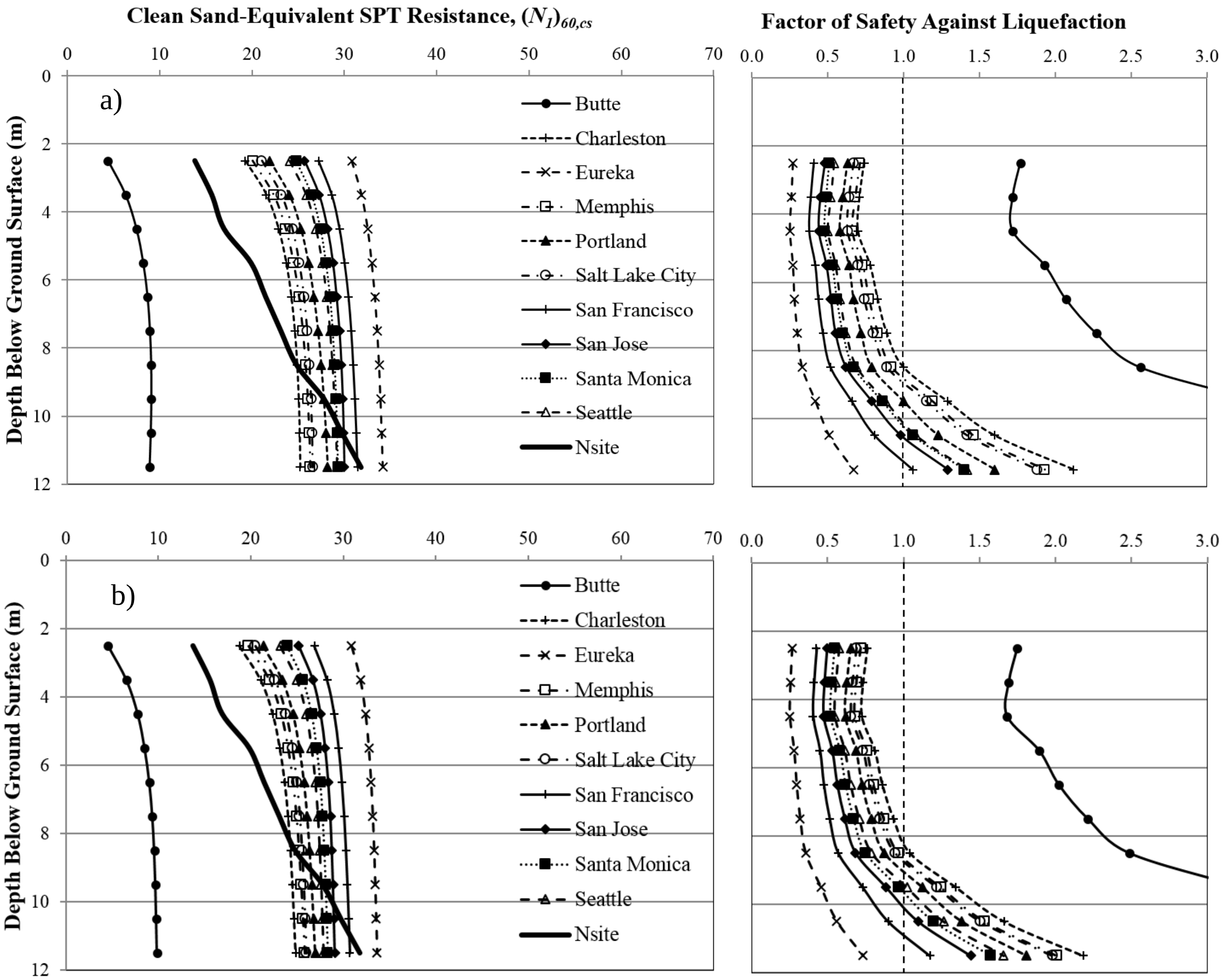

Figure 3.2 N_{req} and FS_L with depth as calculated using a) full performance-based and b) simplified performance-based liquefaction triggering method (T_R = 1,033 years)

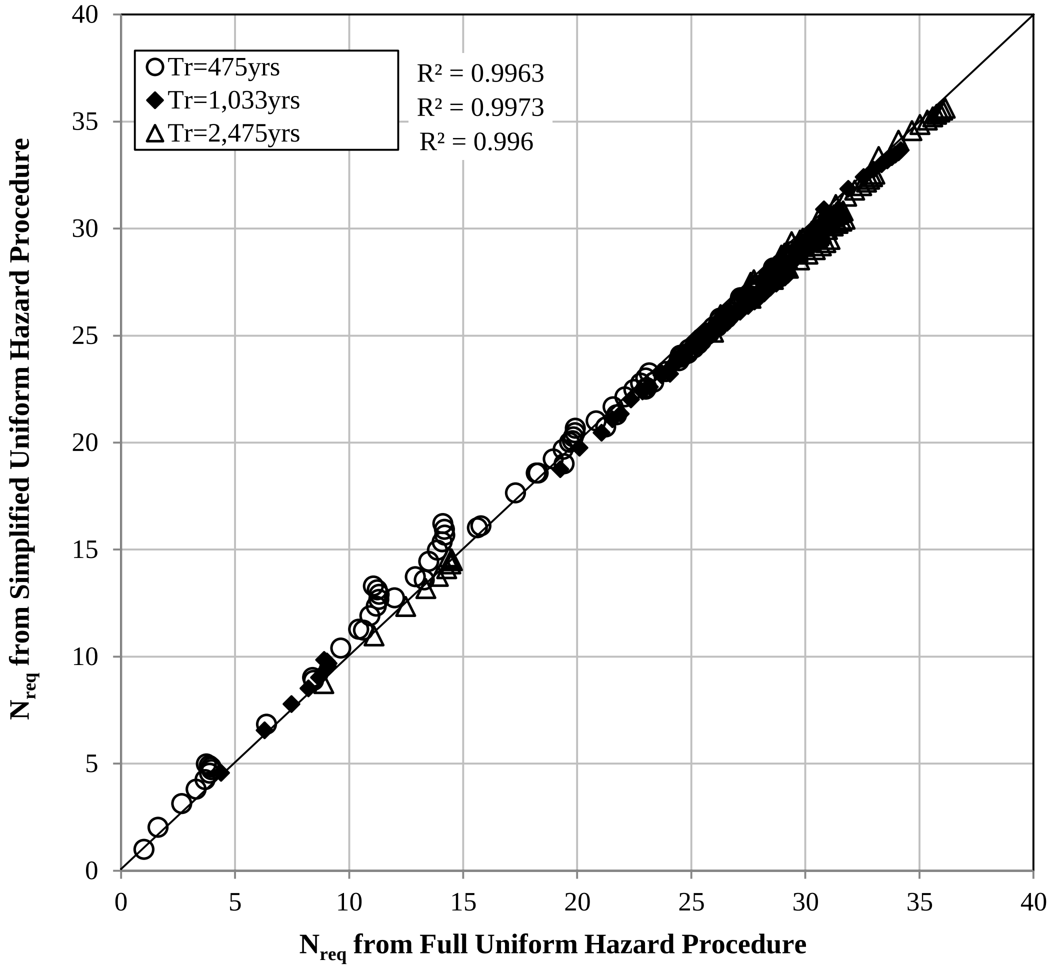

Figure 3.3 Comparison of N_{req} values for the simplified and full performance-based models

3.3 Simplified Lateral Spread Displacement Model Validation

To evaluate the site-specific lateral displacement, a soil profile was assumed for each site. These soil parameters are presented in Figure 3.4. Values of 1.0m, 25%, and 1.0mm were computed for the lateral spread parameters T_{15}, F_{15}, and $D50_{15}$, respectively. As shown in Figure 3.4, the geometry of the site constitutes a ground slope condition with ground slope (i.e. S) equal to 1%. The resulting value of $\mathscr{S}$ for the site, as computed from Equation (51), is therefore equal to 9.846.

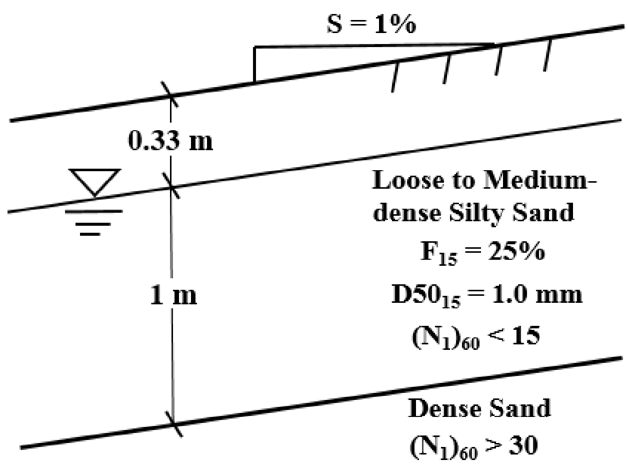

Figure 3.4 Site-specific soil profile used in the simplified lateral spread displacement model validation

3.3.1 EZ-FRISK

To perform the site-specific analysis for both the simplified and full performance-based models, the software EZ-FRISK (Risk Engineering 2013) was utilized. For this analysis, the USGS 2008 seismic source model (Petersen et al. 2008) was used for all locations but Anchorage, Alaska. The 1996 USGS seismic source model was used for that location.

3.3.2 Comparison of Results

Using EZ-FRISK and the soil profile selected for the site specific analysis, the lateral spread displacement was determined for each site using the simplified and full-performance based models. The results of analysis can be seen in Table 3.2. As can be seen in this table, the results of the analysis for both models resulted in relatively similar results, with the values from the simplified method falling on average within 3.9% of those predicted by full model. The observed discrepancy between the simplified and full performance-based models was no greater than 0.073 m at any site or any return period.

Table 3.2 Lateral spread displacements (m) for the site specific analysis using the two models for the three desired return periods

	Simplified Model			Full PB Model		
Site	**475 Yrs**	**1033 Yrs**	**2475 Yrs**	**475 Yrs**	**1033 Yrs**	**2475 Yrs**
Butte	0.001	0.003	0.008	0.001	0.003	0.008
Charleston	0.001	0.017	0.068	0.001	0.015	0.065
Eureka	0.738	2.321	3.737	0.728	2.248	3.724
Memphis	0.003	0.033	0.067	0.003	0.025	0.065
Portland	0.038	0.152	0.333	0.036	0.152	0.334
Salt Lake City	0.162	0.437	0.726	0.167	0.438	0.726
San Francisco	0.744	1.095	1.493	0.745	1.081	1.492
San Jose	0.312	0.574	0.857	0.312	0.574	0.857
Santa Monica	0.171	0.400	0.719	0.172	0.400	0.719
Seattle	0.054	0.162	0.343	0.053	0.162	0.344
Anchorage	0.045	0.536	1.187	0.045	0.566	1.250

Overall, the difference between the simplified and full performance based model is within an acceptable amount of error (defined by this report as 5%). The closeness of the fit is apparent when the results of both analyses are plotted against each other, which can be seen in Figure 3.5 (these are actual displacement values, not averages). The R^2 values for each return period are larger than 0.9995, indicating that the approximation of the full method is very good. These high R^2 values, as well as the lack of scatter of the results, seem to be too close for a simplified method; however, because this is a mathematically derived relationship it is expected that the results be closely correlated with those of the full probabilistic analysis. If the fit was not so close, than the mathematically derived equation would be suspect.

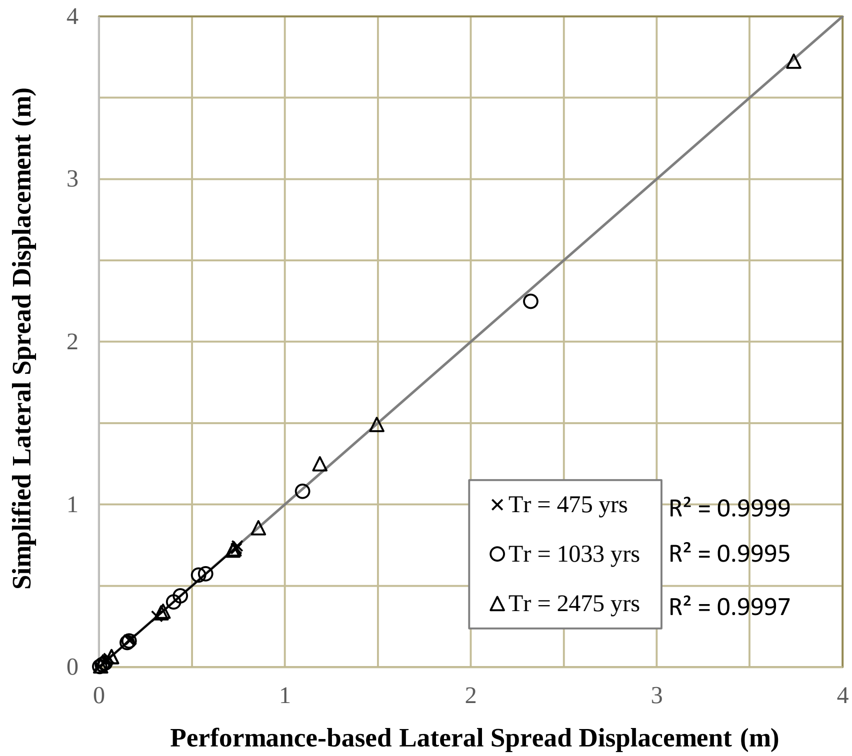

Figure 3.5 Comparison of lateral spread displacements for the simplified and full performance-based models

3.4 Summary

Ten sites throughout the United States were analyzed using both the full and simplified probabilistic procedures for three different return periods: 475, 1033, and 2475 years. Both the simplified liquefaction triggering method and the simplified lateral spread displacement models provided reasonable approximations of their respective full probabilistic methods.

4.0 CONCLUSIONS

4.1 Summary

The purpose of the research being performed is to provide the benefit of the full performance-based probabilistic earthquake hazard analysis, without requiring special software, training, and experience. To accomplish this goal, simplified models of liquefaction triggering and lateral spread displacements were developed that reasonably approximate the results of full performance-based analyses. The objective of this report was to introduce the original models used to determine earthquake hazards (i.e. liquefaction triggering and lateral spread displacement), provide in-depth derivations that demonstrate the development of the simplified methods, and then validate the simplified models by performing a site-specific analysis for several different sites using the simplified and full models.

4.2 Findings

4.2.1 Derivation of the Simplified Procedures

The derivations of the simplified liquefaction triggering and lateral spread displacement models show how to approximate a full performance-based analysis using simple calculations and mapped reference parameters. The simplified liquefaction triggering procedure is based on the Boulanger and Idriss (2012) probabilistic model while the simplified lateral spread displacement model is based on the Youd et al. (2002) empirical model.

4.2.2 Validation of the Simplified Procedures

Ten sites throughout the United States were analyzed using both the full and simplified probabilistic procedures for three different return periods: 475, 1033, and 2475 years. Both the simplified liquefaction triggering method and the simplified lateral spread displacement models provided reasonable approximations of their respective full probabilistic methods. This shows that the simplified procedures derived in this report can be used to approximate the results of a full probabilistic procedure without the need for special software, training, and experience.

4.3 Limitations and Challenges

During the production of this report, a revised Boulanger and Idriss (2014) model was published. This revised model included a new definition of the *MSF* (as explained previously). Though this report discussed the derivation of the simplified performance-based procedure for both the updated Boulanger and Idriss (2014) model and the previous Boulanger and Idriss (2012) model, the software performing the calculations for this mapping study (PBLiquefY) was not able to be updated in time to use the 2014 version of the *MSF* in the validation calculations. Hence, the validation of the simplified Boulanger and Idriss performance-based liquefaction triggering model in this report was performed using the 2012 version of the *MSF*. During the next quarter, the software will be updated to include the option of using the 2014 *MSF* term.

REFERENCES

Bartlett, S.F., and Youd, T.L. (1995). Empirical prediction of liquefaction-induced lateral spread. *J. Geotech. Eng.*, 121(4), 316-329.

Boulanger, R. W., and Idriss, I. M. (2012). Probabilistic standard penetration test-based liquefaction-triggering procedure. *J. Geotech. Geoenviron. Eng.*, 10.1061/(ASCE)GT.1943-5606.0000700, 1185–1195.

Boulanger, R. W., and Idriss, I. M. (2014). CPT and SPT based liquefaction triggering procedures. *Rep. UCD/CGM-14/01*, Dept. of Civil and Environmental Engineering, Univ. of California–Davis, Davis, CA.

Cetin, K. O., et al. (2004). Standard penetration test-based probabilistic and deterministic assessment of seismic soil liquefaction potential. *J. Geotech. Geoenviron. Eng*., 10.1061/(ASCE)1090-0241(2004)130:12(1314), 1314–1340.

Cornell, C.A., and Krawinkler, H. (2000). Progress and challenges in seismic performance assessment. *PEER News*, April, 1-3.Deierlein, G.G., Krawinkler, H., and Cornell, C.A. (2003). A framework for performance-based earthquake engineering, Proc., 2003 Pacific Conference on Earthquake Engineering.

Franke, K. and Wright, A. (2013) An Alternative Performance-Based Liquefaction Initiation Procedure for the Standard Penetration Test. *Geo-Congress 2013*, 10.1061/9780784412787.086, 846-849.

Franke, K.W. and Kramer, S.L. (2014). A procedure for the empirical evaluation of lateral spread displacement hazard curves. *J. Geotech. Geoenviron. Eng.*, ASCE, 140(1), 110-120.

Franke, K.W., Lingwall, B.N., Youd, T.L. (2014a). Sensitivity of empirical liquefaction assessment to seismic loading in areas of low seismicity and its implications for sustainability, Geo-Congress 2014 Technical Papers, p. 1284-1293.

Franke, K., Wright, A., and Ekstrom, L. (2014b). Comparative Study between Two Performance-Based Liquefaction Triggering Models for the Standard Penetration Test. *J. Geotech. Geoenviron. Eng.* , 10.1061/(ASCE)GT.1943-5606.0001094 , 04014010.

Franke, K.W., Wright, A.D., and Hatch, C.K. (2014c). PBLiquefY: A new analysis tool for the performance-based evaluation of liquefaction triggering. Proceedings, 10^{th} National Conference on Earthquake Engineering, Paper No. 87, EERI, Oakland, CA.

Franke, K.W., Mayfield, R.T., and Wright, A.D. (2014d). Simplified uniform hazard analysis for bridges, *Transportation Research Record*, TRB, in press, Washington D.C.

Idriss, I.M., and Boulanger, R.W. (2008). *Soil liquefaction during earthquakes.* Monograph MNO-12, Earthquake Engineering Research Institute, Oakland, CA 261 pp.

Idriss, I. M., and Boulanger, R. W. (2010). SPT-based liquefaction triggering procedures. *Rep. UCD/CGM-10/02*, Dept. of Civil and Environmental Engineering, Univ. of California–Davis, Davis, CA.

Kramer, S.L. (2008). Evaluation of liquefaction hazards in Washington State. WSDOT Report WA-RD 668.1, 152 pp.

Kramer, S.K., Franke, K.W., Huang, Y.-M., and Baska, D. (2007). Performance-based evaluation of lateral spreading displacement. *Proceedings, 4th International Conference on Earthquake Geotechnical Engineering*, Paper No. 1208, Thessaloniki, Greece, June 2007.

Krawinkler, H. (2002). A general approach to seismic performance assessment, Proc., Int. Conf. on Advances and New Challenges in Earthquake Engineering Research, ICANCEER, Hong Kong.

Mayfield, R. T., Kramer, S. L., and Huang, Y.-M. (2010). Simplified approximation procedure for performance-based evaluation of liquefaction potential. *J. Geotech. Geoenviron. Eng*., 10.1061/(ASCE) GT.1943-5606.0000191, 140–150.

Petersen, Mark D., Frankel, Arthur D., Harmsen, Stephen C., Mueller, Charles S., Haller, Kathleen M., Wheeler, Russell L., Wesson, Robert L., Zeng, Yuehua, Boyd, Oliver S., Perkins, David M., Luco, Nicolas, Field, Edward H., Wills, Chris J., and Rukstales, Kenneth S. (2008). Documentation for the 2008 Update of the United States National Seismic Hazard Maps. Open-File Report 2008–1128, United States Geological Survey, Denver, CO: available at website: http://pubs.usgs.gov/of/2008/1128/.

Risk Engineering. (2013). EZ-FRISK, ver. 7.60. Boulder, Colorado.

Seed, H.B. (1979). Soil liquefaction and cyclic mobility evaluation for level ground during earthquakes. *J. Geotech. Eng. Div*., 105(GT2), p. 201-255.

Seed, H.B. and Idriss, I.M. (1971). Simplified procedure for evaluating soil liquefaction potential," *J. Soil Mech. and Found. Div*., 97(SM9), p. 1249-1273.

Seed, H.B. and Idriss, I.M. (1982). *Ground Motions and Soil Liquefaction During Earthquakes*. EERI, Oakland, CA, 134 pp.

Seed, H.B., Tokimatsu, K., Harder, L.F. Jr., and Chung, R. (1985). Influence of SPT procedures in soil liquefaction resistance evaluations, *J. Geotech. Eng*., 111(12), p. 1425-1445.

Stewart, J.P., Liu, A.H., and Choi, Y. (2003). Amplification factors for spectral acceleration in tectonically active regions. *Bull. Seismol. Soc. Am.*, 93(7): 332-352.

USGS. (2008). “USGS 2008 interactive deaggregation.” https://geohazards.usgs.gov/deaggint/2008/ (March 26, 2014).

Youd, T.L., Hansen, C.M., and Bartlett, S.F. (2002). Revised multilinear regression equations for prediction of lateral spread displacement. *J. Geotech. Geoenviron. Eng.,* ASCE. 128(12), 1007-1017.

APPENDIX A: Supplementary Validation Data

The following tables are supplementary to the validation results of this report but are too lengthy to include in the body of the text. The values in Table A.1 are values used in the calculation of CSR^{site} for each of the ten cities in the study. The values of $\%CSR^{ref}$ were retrieved from the hazard-targeted liquefaction parameter maps created using PBLiquefY. The values of mean M and PGA were retrieved from the 2008 USGS deaggregation website. Values of F_{pga} were retrieved from AASHTO 2012 Table 3.10.3.2-1. Table A.2 displays the results of the simplified liquefaction triggering procedure while Table A.3 displays the results of the full probabilistic liquefaction triggering procedure.

Depth conversions: 2.5 m (8.20 ft), 3.5 m (11.48 ft), 4.5 m (14.76 ft), 5.5 m (18.04 ft), 6.5 m (21.33 ft), 7.5 m (24.61 ft), 8.5 m (27.89 ft), 9.5 m (31.17 ft), 10.5 m (34.45 ft), 11.5 m (37.73 ft)

Table A.1 Parameters Used in Simplified Liquefaction Triggering Procedure

Location	T_R = 1033				T_R = 475				T_R = 2475			
	$\%CSR^{ref}$	Mean M	PGA	F_{pga}	$\%CSR^{ref}$	Mean M	PGA	F_{pga}	$\%CSR^{ref}$	Mean M	PGA	F_{pga}
Butte	10.37	6.03	0.1206	1.559	7.434	6.03	0.0834	1.600	14.671	6.05	0.1785	1.443
Charleston	33.46	6.87	0.3680	1.132	12.750	6.61	0.1513	1.497	66.794	7.00	0.7287	1.000
Eureka	109.64	7.40	0.9662	1.000	67.819	7.33	0.6154	1.000	162.159	7.45	1.4004	1.000
Memphis	34.73	7.19	0.3346	1.165	14.811	6.98	0.1604	1.479	61.245	7.24	0.5711	1.000
Portland	37.08	7.29	0.2980	1.204	23.485	7.24	0.1990	1.402	55.225	7.31	0.4366	1.063
Salt Lake City	38.09	6.84	0.4030	1.097	20.724	6.75	0.2126	1.375	62.332	6.90	0.6717	1.000
San Francisco	68.49	7.38	0.5685	1.000	50.860	7.31	0.4394	1.061	90.113	7.44	0.7254	1.000
San Jose	57.89	6.67	0.5627	1.000	45.322	6.66	0.4560	1.044	72.345	6.66	0.6911	1.000
Santa Monica	52.70	6.79	0.5372	1.000	37.984	6.74	0.3852	1.115	71.788	6.84	0.7415	1.000
Seattle	47.29	6.82	0.4444	1.056	32.213	6.75	0.3110	1.189	67.879	6.88	0.6432	1.000

Table A.2 Results from Simplified Liquefaction Triggering Procedure

		T_R = 1033 Simple PB (Idriss & Boulanger)				T_R = 475 Simple PB (Idriss & Boulanger)				T_R = 2475 Simple PB (Idriss & Boulanger)			
	Depth (m)	$N_{1,60,cs}$ site	N_{req}	$\%CSR^{site}$	FS_L	P_L	N_{req}	$\%CSR^{site}$	FS_L	P_L	N_{req}	$\%CSR^{site}$	FS_L	P_L
Butte	2.5	13.78	4.568	9.528	1.747	0.022	1.000	7.434	2.375	0.002	8.740	12.467	1.335	0.148
	3.5	15.62	6.554	10.867	1.691	0.029	2.029	7.994	2.299	0.001	10.965	14.223	1.292	0.177
	4.5	16.95	7.780	11.749	1.681	0.030	3.144	8.642	2.285	0.001	12.344	15.377	1.284	0.183
	5.5	19.87	8.522	12.301	1.892	0.011	3.811	9.049	2.572	0.000	13.178	16.104	1.445	0.092
	6.5	21.47	9.030	12.688	2.021	0.006	4.266	9.335	2.748	0.000	13.749	16.615	1.544	0.059
	7.5	23.12	9.356	12.940	2.213	0.002	4.553	9.518	3.008	0.000	14.111	16.945	1.690	0.029
	8.5	24.83	9.553	13.094	2.487	0.001	4.729	9.633	3.381	0.000	14.336	17.153	1.899	0.010
	9.5	27.79	9.685	13.197	3.238	0.000	4.846	9.709	4.401	0.000	14.484	17.291	2.471	0.001
	10.5	29.76	9.772	13.265	4.036	0.000	4.921	9.757	5.486	0.000	14.581	17.382	3.080	0.000
	11.5	31.81	9.848	13.325	5.346	0.000	4.990	9.803	7.268	0.000	14.669	17.465	4.079	0.000
Charleston	2.5	13.78	18.765	21.832	0.762	0.836	6.850	11.076	1.503	0.071	26.706	38.365	0.434	0.999
	3.5	15.62	21.090	25.043	0.734	0.868	9.023	12.683	1.449	0.090	28.077	44.043	0.417	0.999
	4.5	16.95	22.393	27.241	0.725	0.877	10.406	13.769	1.434	0.097	28.842	47.955	0.412	0.999
	5.5	19.87	23.158	28.716	0.810	0.776	11.284	14.485	1.606	0.044	29.299	50.607	0.460	0.997
	6.5	21.47	23.688	29.836	0.860	0.708	11.919	15.016	1.708	0.027	29.620	52.638	0.487	0.995
	7.5	23.12	24.052	30.657	0.934	0.597	12.362	15.393	1.860	0.013	29.846	54.151	0.529	0.989
	8.5	24.83	24.312	31.273	1.041	0.442	12.676	15.664	2.079	0.004	30.011	55.306	0.589	0.972
	9.5	27.79	24.519	31.781	1.344	0.143	12.921	15.878	2.691	0.000	30.145	56.276	0.759	0.840
	10.5	29.76	24.691	32.215	1.662	0.033	13.120	16.053	3.335	0.000	30.259	57.122	0.937	0.593
	11.5	31.81	24.855	32.643	2.182	0.002	13.310	16.221	4.392	0.000	30.368	57.957	1.229	0.228
Eureka	2.5	13.78	30.898	62.315	0.267	1.000	26.775	38.616	0.431	0.999	33.360	92.041	0.181	1.000
	3.5	15.62	31.855	71.732	0.256	1.000	28.158	44.432	0.414	0.999	34.124	105.987	0.173	1.000
	4.5	16.95	32.412	78.334	0.252	1.000	28.938	48.494	0.407	0.999	34.576	115.783	0.171	1.000
	5.5	19.87	32.757	82.929	0.281	1.000	29.413	51.310	0.454	0.998	34.860	122.624	0.190	1.000
	6.5	21.47	33.008	86.554	0.296	1.000	29.754	53.520	0.479	0.996	35.069	128.038	0.200	1.000
	7.5	23.12	33.193	89.368	0.320	1.000	30.000	55.226	0.518	0.991	35.223	132.260	0.216	1.000
	8.5	24.83	33.334	91.620	0.355	1.000	30.187	56.581	0.576	0.977	35.342	135.660	0.240	1.000
	9.5	27.79	33.453	93.596	0.457	0.998	30.343	57.761	0.740	0.862	35.443	138.653	0.308	1.000
	10.5	29.76	33.559	95.388	0.561	0.981	30.479	58.825	0.910	0.633	35.533	141.378	0.379	1.000
	11.5	31.81	33.661	97.183	0.733	0.869	30.611	59.888	1.190	0.265	35.620	144.113	0.494	0.995
Memphis	2.5	13.78	19.764	23.120	0.720	0.882	8.898	12.588	1.322	0.157	25.676	34.955	0.476	0.996
	3.5	15.62	22.022	26.578	0.692	0.909	11.242	14.450	1.272	0.193	27.188	40.195	0.457	0.998
	4.5	16.95	23.285	28.978	0.681	0.917	12.754	15.731	1.255	0.206	28.034	43.841	0.450	0.998
	5.5	19.87	24.039	30.628	0.760	0.839	13.730	16.598	1.402	0.111	28.543	46.355	0.502	0.994
	6.5	21.47	24.570	31.908	0.804	0.785	14.452	17.261	1.486	0.076	28.906	48.315	0.531	0.989
	7.5	23.12	24.946	32.882	0.871	0.691	14.974	17.755	1.613	0.042	29.166	49.812	0.575	0.977
	8.5	24.83	25.225	33.645	0.968	0.547	15.361	18.129	1.796	0.017	29.361	50.991	0.639	0.947
	9.5	27.79	25.454	34.299	1.246	0.214	15.681	18.444	2.317	0.001	29.523	52.009	0.822	0.761
	10.5	29.76	25.652	34.882	1.535	0.061	15.955	18.718	2.860	0.000	29.663	52.918	1.012	0.483
	11.5	31.81	25.841	35.461	2.009	0.006	16.220	18.986	3.752	0.000	29.799	53.825	1.324	0.156

		T_R = 1033 Simple PB (Idriss & Boulanger)				T_R = 475 Simple PB (Idriss & Boulanger)				T_R = 2475 Simple PB (Idriss & Boulanger)			
	Depth (m)	$N_{1,60,cs}$ site	N_{req}	$\%CSR^{site}$	FS_L	P_L	N_{req}	$\%CSR^{site}$	FS_L	P_L	N_{req}	$\%CSR^{site}$	FS_L	P_L
Portland	2.5	13.78	21.346	25.447	0.654	0.937	16.028	18.792	0.886	0.669	25.152	33.443	0.498	0.994
	3.5	15.62	23.426	29.272	0.628	0.954	18.582	21.609	0.851	0.721	26.736	38.474	0.478	0.996
	4.5	16.95	24.583	31.940	0.618	0.959	20.091	23.570	0.838	0.739	27.621	41.987	0.470	0.997
	5.5	19.87	25.274	33.783	0.689	0.911	21.011	24.920	0.934	0.598	28.155	44.417	0.524	0.990
	6.5	21.47	25.765	35.227	0.728	0.874	21.668	25.975	0.987	0.518	28.537	46.324	0.554	0.984
	7.5	23.12	26.116	36.336	0.788	0.805	22.137	26.780	1.069	0.405	28.812	47.790	0.599	0.968
	8.5	24.83	26.379	37.213	0.875	0.685	22.486	27.413	1.188	0.267	29.019	48.953	0.665	0.929
	9.5	27.79	26.597	37.974	1.125	0.335	22.775	27.960	1.528	0.063	29.192	49.965	0.855	0.714
	10.5	29.76	26.786	38.657	1.385	0.120	23.025	28.449	1.882	0.011	29.342	50.874	1.052	0.427
	11.5	31.81	26.968	39.341	1.811	0.016	23.265	28.937	2.462	0.001	29.488	51.785	1.376	0.125
Salt Lake City	2.5	13.78	20.465	24.103	0.691	0.909	13.594	16.475	1.010	0.485	25.979	35.895	0.464	0.997
	3.5	15.62	22.608	27.641	0.665	0.930	16.118	18.883	0.973	0.539	27.431	41.183	0.446	0.998
	4.5	16.95	23.789	30.059	0.657	0.935	17.651	20.521	0.962	0.555	28.235	44.806	0.441	0.998
	5.5	19.87	24.479	31.680	0.735	0.867	18.585	21.613	1.077	0.395	28.712	47.246	0.493	0.995
	6.5	21.47	24.955	32.906	0.779	0.816	19.242	22.432	1.143	0.314	29.044	49.099	0.522	0.990
	7.5	23.12	25.282	33.804	0.847	0.726	19.694	23.025	1.244	0.216	29.275	50.466	0.567	0.980
	8.5	24.83	25.513	34.472	0.945	0.581	20.012	23.460	1.388	0.118	29.442	51.493	0.632	0.951
	9.5	27.79	25.698	35.022	1.220	0.236	20.263	23.812	1.794	0.017	29.576	52.346	0.816	0.768
	10.5	29.76	25.851	35.491	1.508	0.069	20.470	24.109	2.220	0.002	29.687	53.078	1.009	0.488
	11.5	31.81	25.996	35.950	1.982	0.007	20.667	24.399	2.920	0.000	29.795	53.798	1.324	0.155
San Francisco	2.5	13.78	26.864	38.946	0.427	0.999	24.088	30.742	0.541	0.987	29.389	51.161	0.325	1.000
	3.5	15.62	28.240	44.826	0.410	0.999	25.811	35.367	0.520	0.991	30.490	58.910	0.312	1.000
	4.5	16.95	29.017	48.943	0.403	0.999	26.769	38.596	0.512	0.992	31.124	64.350	0.307	1.000
	5.5	19.87	29.491	51.807	0.449	0.998	27.346	40.831	0.570	0.979	31.516	68.146	0.341	1.000
	6.5	21.47	29.833	54.061	0.474	0.996	27.757	42.583	0.602	0.966	31.802	71.150	0.360	1.000
	7.5	23.12	30.081	55.810	0.513	0.992	28.053	43.931	0.652	0.939	32.011	73.488	0.390	1.000
	8.5	24.83	30.270	57.205	0.569	0.979	28.275	45.000	0.724	0.878	32.171	75.370	0.432	0.999
	9.5	27.79	30.429	58.427	0.731	0.871	28.460	45.929	0.930	0.603	32.307	77.025	0.555	0.983
	10.5	29.76	30.568	59.533	0.899	0.649	28.622	46.766	1.145	0.313	32.427	78.532	0.682	0.917
	11.5	31.81	30.702	60.642	1.175	0.280	28.777	47.602	1.497	0.073	32.544	80.043	0.890	0.663
San Jose	2.5	13.78	25.188	33.542	0.496	0.994	22.491	27.421	0.607	0.964	27.607	41.926	0.397	1.000
	3.5	15.62	26.722	38.422	0.478	0.996	24.368	31.409	0.585	0.973	28.854	48.023	0.383	1.000
	4.5	16.95	27.562	41.734	0.473	0.997	25.390	34.113	0.579	0.976	29.546	52.158	0.379	1.000
	5.5	19.87	28.051	43.924	0.530	0.989	25.981	35.900	0.648	0.941	29.953	54.892	0.424	0.999
	6.5	21.47	28.387	45.558	0.563	0.981	26.385	37.232	0.689	0.911	30.233	56.928	0.451	0.998
	7.5	23.12	28.614	46.728	0.613	0.961	26.656	38.185	0.750	0.851	30.423	58.385	0.490	0.995
	8.5	24.83	28.773	47.576	0.685	0.914	26.845	38.875	0.838	0.739	30.556	59.438	0.548	0.985
	9.5	27.79	28.895	48.252	0.886	0.670	26.991	39.425	1.084	0.386	30.659	60.278	0.709	0.893
	10.5	29.76	28.995	48.814	1.097	0.370	27.108	39.880	1.342	0.144	30.742	60.975	0.878	0.681
	11.5	31.81	29.089	49.359	1.443	0.093	27.220	40.320	1.767	0.020	30.821	61.649	1.156	0.301

			T_R = 1033 Simple PB (Idriss & Boulanger)				T_R = 475 Simple PB (Idriss & Boulanger)				T_R = 2475 Simple PB (Idriss & Boulanger)			
	Depth (m)	$N_{1,60,cs}$ site	N_{req}	$\%CSR^{site}$	FS_L	P_L	N_{req}	$\%CSR^{site}$	FS_L	P_L	N_{req}	$\%CSR^{site}$	FS_L	P_L
Santa Monica	2.5	13.78	23.956	30.437	0.547	0.985	20.730	24.493	0.680	0.918	27.485	41.406	0.402	0.999
	3.5	15.62	25.656	34.894	0.527	0.990	22.832	28.070	0.655	0.937	28.756	47.486	0.387	1.000
	4.5	16.95	26.586	37.933	0.521	0.991	23.985	30.504	0.647	0.942	29.465	51.641	0.382	1.000
	5.5	19.87	27.130	39.964	0.582	0.975	24.655	32.124	0.724	0.878	29.886	54.427	0.428	0.999
	6.5	21.47	27.505	41.493	0.618	0.959	25.114	33.338	0.769	0.828	30.180	56.534	0.454	0.998
	7.5	23.12	27.762	42.606	0.672	0.924	25.426	34.217	0.837	0.740	30.384	58.076	0.493	0.995
	8.5	24.83	27.944	43.427	0.750	0.851	25.644	34.860	0.934	0.597	30.529	59.225	0.550	0.985
	9.5	27.79	28.088	44.098	0.969	0.545	25.816	35.382	1.208	0.248	30.645	60.169	0.710	0.892
	10.5	29.76	28.207	44.666	1.199	0.257	25.955	35.818	1.495	0.073	30.742	60.973	0.878	0.681
	11.5	31.81	28.320	45.220	1.575	0.050	26.088	36.244	1.966	0.007	30.835	61.763	1.153	0.303
Seattle	2.5	13.78	23.208	28.820	0.578	0.976	19.016	22.145	0.752	0.849	26.908	39.111	0.426	0.999
	3.5	15.62	25.007	33.047	0.556	0.983	21.304	25.380	0.724	0.878	28.247	44.864	0.410	0.999
	4.5	16.95	25.991	35.934	0.550	0.985	22.577	27.583	0.716	0.886	28.993	48.806	0.405	0.999
	5.5	19.87	26.566	37.864	0.615	0.961	23.320	29.050	0.801	0.788	29.436	51.455	0.452	0.998
	6.5	21.47	26.964	39.323	0.652	0.939	23.830	30.151	0.851	0.720	29.745	53.465	0.480	0.996
	7.5	23.12	27.237	40.389	0.709	0.893	24.176	30.948	0.925	0.611	29.960	54.942	0.521	0.991
	8.5	24.83	27.431	41.180	0.791	0.801	24.419	31.533	1.033	0.454	30.114	56.050	0.581	0.975
	9.5	27.79	27.584	41.828	1.022	0.469	24.610	32.008	1.335	0.148	30.238	56.967	0.750	0.850
	10.5	29.76	27.711	42.380	1.263	0.200	24.765	32.406	1.652	0.035	30.342	57.752	0.927	0.608
	11.5	31.81	27.833	42.920	1.660	0.034	24.913	32.795	2.172	0.003	30.441	58.524	1.217	0.239

Table A.3 Results from Full Probabilistic Liquefaction Triggering Procedure

			T_R = 1033 Full PB (Idriss & Boulanger)				T_R = 475 Full PB (Idriss & Boulanger)				T_R = 2475 Full PB (Idriss & Boulanger)			
	Depth (m)	$N_{1,60,cs}$ site	N_{req}	$\%CSR^{site}$	FS_L	P_L	N_{req}	$\%CSR^{site}$	FS_L	P_L	N_{req}	$\%CSR^{site}$	FS_L	P_L
Butte	2.5	13.78	4.38	9.408	1.77	0.020	1	7.434	2.24	0.002	8.89	12.581	1.32	0.156
	3.5	15.62	6.29	10.682	1.72	0.025	1.62	7.767	2.37	0.001	11.09	14.325	1.28	0.184
	4.5	16.95	7.47	11.522	1.72	0.026	2.65	8.350	2.37	0.001	12.47	15.486	1.28	0.190
	5.5	19.87	8.21	12.067	1.93	0.009	3.29	8.730	2.67	0.000	13.36	16.266	1.43	0.098
	6.5	21.47	8.68	12.421	2.07	0.004	3.68	8.968	2.86	0.000	13.91	16.761	1.53	0.062
	7.5	23.12	8.94	12.619	2.27	0.002	3.88	9.092	3.15	0.000	14.27	17.092	1.68	0.031
	8.5	24.83	9.07	12.719	2.56	0.000	3.96	9.142	3.56	0.000	14.46	17.269	1.89	0.011
	9.5	27.79	9.09	12.735	3.36	0.000	3.95	9.136	4.68	0.000	14.52	17.325	2.47	0.001
	10.5	29.76	9.02	12.681	4.22	0.000	3.87	9.086	5.89	0.000	14.48	17.287	3.10	0.000
	11.5	31.81	8.9	12.589	5.66	0.000	3.73	8.999	7.92	0.000	14.37	17.185	4.15	0.000
Charleston	2.5	13.78	19.25	22.443	0.74	0.860	6.38	10.745	1.55	0.057	26.94	39.232	0.42	0.999
	3.5	15.62	21.54	25.762	0.71	0.889	8.39	12.202	1.51	0.070	28.37	45.472	0.40	0.999
	4.5	16.95	22.85	28.104	0.70	0.899	9.63	13.154	1.50	0.071	29.2	50.012	0.39	1.000
	5.5	19.87	23.68	29.819	0.78	0.815	10.42	13.781	1.69	0.029	29.75	53.497	0.44	0.999
	6.5	21.47	24.23	31.076	0.83	0.756	10.9	14.170	1.81	0.016	30.13	56.163	0.46	0.998
	7.5	23.12	24.6	31.984	0.89	0.655	11.18	14.399	1.99	0.007	30.41	58.281	0.49	0.995
	8.5	24.83	24.86	32.654	1.00	0.504	11.3	14.498	2.25	0.002	30.61	59.879	0.54	0.986
	9.5	27.79	25.03	33.108	1.29	0.179	11.31	14.507	2.95	0.000	30.76	61.127	0.70	0.902
	10.5	29.76	25.13	33.381	1.60	0.044	11.22	14.432	3.71	0.000	30.86	61.984	0.86	0.702
	11.5	31.81	25.19	33.547	2.12	0.003	11.06	14.300	4.98	0.000	30.94	62.684	1.14	0.322
Eureka	2.5	13.78	30.81	61.553	0.27	1.000	27.15	40.044	0.42	0.999	33.2	89.482	0.19	1.000
	3.5	15.62	31.88	72.010	0.26	1.000	28.59	46.600	0.39	1.000	34.08	105.096	0.18	1.000
	4.5	16.95	32.55	80.128	0.25	1.000	29.44	51.481	0.38	1.000	34.66	117.738	0.17	1.000
	5.5	19.87	32.98	86.133	0.27	1.000	30	55.225	0.42	0.999	35.02	126.741	0.18	1.000
	6.5	21.47	33.33	91.557	0.28	1.000	30.4	58.203	0.44	0.998	35.34	135.607	0.19	1.000
	7.5	23.12	33.58	95.759	0.30	1.000	30.7	60.622	0.47	0.997	35.58	142.853	0.20	1.000
	8.5	24.83	33.78	99.337	0.33	1.000	30.93	62.596	0.52	0.991	35.75	148.324	0.22	1.000
	9.5	27.79	33.93	102.156	0.42	0.999	31.11	64.217	0.67	0.929	35.89	153.055	0.28	1.000
	10.5	29.76	34.07	104.896	0.51	0.992	31.25	65.527	0.82	0.767	36.01	157.281	0.34	1.000
	11.5	31.81	34.18	107.127	0.67	0.930	31.36	66.588	1.07	0.404	36.13	161.673	0.44	0.998
Memphis	2.5	13.78	20.09	23.568	0.71	0.895	8.43	12.232	1.36	0.133	26.17	36.513	0.46	0.998
	3.5	15.62	22.35	27.163	0.68	0.921	10.62	13.942	1.32	0.159	27.73	42.462	0.43	0.999
	4.5	16.95	23.66	29.775	0.66	0.931	11.99	15.076	1.31	0.165	28.64	46.863	0.42	0.999
	5.5	19.87	24.5	31.733	0.73	0.869	12.9	15.859	1.47	0.083	29.24	50.252	0.46	0.997
	6.5	21.47	25.08	33.244	0.77	0.826	13.49	16.382	1.57	0.053	29.67	52.963	0.48	0.996
	7.5	23.12	25.49	34.403	0.83	0.746	13.87	16.725	1.71	0.026	29.98	55.083	0.52	0.991
	8.5	24.83	25.8	35.334	0.92	0.616	14.08	16.917	1.93	0.009	30.23	56.904	0.57	0.978
	9.5	27.79	26.02	36.025	1.19	0.269	14.18	17.009	2.51	0.000	30.43	58.437	0.73	0.871
	10.5	29.76	26.18	36.546	1.46	0.084	14.17	17.000	3.15	0.000	30.58	59.634	0.90	0.652
	11.5	31.81	26.3	36.946	1.93	0.009	14.1	16.935	4.21	0.000	30.69	60.539	1.18	0.278

		T_R = 1033 Full PB (Idriss & Boulanger)				T_R = 475 Full PB (Idriss & Boulanger)				T_R = 2475 Full PB (Idriss & Boulanger)			
	Depth (m)	$N_{1,60,cs}$ site	N_{req}	$\%CSR^{site}$	FS_L	P_L	N_{req}	$\%CSR^{site}$	FS_L	P_L	N_{req}	$\%CSR^{site}$	FS_L	P_L
Portland	2.5	13.78	21.9	26.367	0.63	0.952	15.62	18.383	0.91	0.640	25.97	35.866	0.46	0.997
	3.5	15.62	24.02	30.584	0.60	0.967	18.2	21.153	0.87	0.694	27.61	41.939	0.44	0.999
	4.5	16.95	25.27	33.771	0.58	0.974	19.78	23.142	0.85	0.717	28.59	46.600	0.42	0.999
	5.5	19.87	26.09	36.251	0.64	0.945	20.82	24.628	0.94	0.581	29.25	50.312	0.46	0.997
	6.5	21.47	26.68	38.271	0.67	0.926	21.56	25.795	0.99	0.508	29.74	53.429	0.48	0.996
	7.5	23.12	27.13	39.965	0.72	0.886	22.09	26.698	1.07	0.400	30.11	56.017	0.51	0.992
	8.5	24.83	27.48	41.387	0.79	0.806	22.48	27.402	1.19	0.266	30.43	58.437	0.56	0.983
	9.5	27.79	27.76	42.595	1.00	0.495	22.77	27.949	1.53	0.063	30.69	60.539	0.71	0.896
	10.5	29.76	27.99	43.638	1.23	0.230	22.99	28.379	1.89	0.011	30.89	62.245	0.86	0.707
	11.5	31.81	28.18	44.537	1.60	0.045	23.15	28.701	2.48	0.001	31.08	63.942	1.11	0.348
Salt Lake City	2.5	13.78	21.06	24.996	0.67	0.929	13.29	16.203	1.03	0.461	26.28	36.878	0.45	0.998
	3.5	15.62	23.18	28.762	0.64	0.947	15.77	18.532	0.99	0.512	27.78	42.684	0.43	0.999
	4.5	16.95	24.38	31.438	0.63	0.953	17.29	20.120	0.98	0.527	28.65	46.916	0.42	0.999
	5.5	19.87	25.13	33.381	0.70	0.904	18.28	21.247	1.10	0.371	29.21	50.072	0.46	0.997
	6.5	21.47	25.65	34.877	0.74	0.866	18.94	22.050	1.16	0.293	29.6	52.504	0.49	0.995
	7.5	23.12	25.99	35.930	0.80	0.794	19.38	22.611	1.27	0.197	29.87	54.314	0.53	0.990
	8.5	24.83	26.24	36.745	0.89	0.668	19.66	22.981	1.42	0.104	30.07	55.727	0.58	0.974
	9.5	27.79	26.41	37.320	1.15	0.313	19.83	23.210	1.84	0.014	30.22	56.829	0.75	0.848
	10.5	29.76	26.52	37.702	1.42	0.103	19.9	23.305	2.30	0.001	30.33	57.662	0.93	0.606
	11.5	31.81	26.58	37.913	1.88	0.011	19.91	23.319	3.06	0.000	30.39	58.125	1.23	0.231
San Francisco	2.5	13.78	27.22	40.322	0.41	0.999	24.51	31.758	0.52	0.990	29.39	51.169	0.33	1.000
	3.5	15.62	28.66	46.969	0.39	1.000	26.25	36.778	0.50	0.994	30.6	59.797	0.31	1.000
	4.5	16.95	29.5	51.861	0.38	1.000	27.26	40.482	0.49	0.995	31.32	66.199	0.30	1.000
	5.5	19.87	30.04	55.511	0.42	0.999	27.91	43.270	0.54	0.987	31.81	71.239	0.33	1.000
	6.5	21.47	30.47	58.752	0.44	0.999	28.38	45.522	0.56	0.981	32.16	75.235	0.34	1.000
	7.5	23.12	30.76	61.127	0.47	0.997	28.71	47.237	0.61	0.965	32.46	78.955	0.36	1.000
	8.5	24.83	30.97	62.950	0.52	0.991	28.95	48.560	0.67	0.925	32.67	81.736	0.40	1.000
	9.5	27.79	31.16	64.680	0.66	0.933	29.15	49.716	0.86	0.708	32.82	83.819	0.51	0.993
	10.5	29.76	31.31	66.102	0.81	0.777	29.3	50.615	1.06	0.420	32.94	85.545	0.63	0.955
	11.5	31.81	31.43	67.278	1.06	0.418	29.41	51.294	1.39	0.118	33.04	87.027	0.82	0.765
San Jose	2.5	13.78	25.67	34.937	0.48	0.996	23	28.399	0.59	0.973	27.74	42.506	0.39	1.000
	3.5	15.62	27.25	40.442	0.45	0.998	24.89	32.734	0.56	0.981	29.08	49.306	0.37	1.000
	4.5	16.95	28.16	44.441	0.44	0.998	25.95	35.803	0.55	0.984	29.88	54.383	0.36	1.000
	5.5	19.87	28.75	47.453	0.49	0.995	26.64	38.127	0.61	0.963	30.44	58.516	0.40	1.000
	6.5	21.47	29.15	49.716	0.52	0.992	27.09	39.809	0.64	0.944	30.79	61.382	0.42	0.999
	7.5	23.12	29.46	51.607	0.55	0.983	27.41	41.095	0.70	0.904	31.04	63.578	0.45	0.998
	8.5	24.83	29.67	52.963	0.62	0.960	27.63	42.026	0.77	0.821	31.28	65.814	0.50	0.994
	9.5	27.79	29.82	53.971	0.79	0.800	27.78	42.684	1.00	0.498	31.45	67.478	0.63	0.950
	10.5	29.76	29.92	54.662	0.98	0.530	27.88	43.133	1.24	0.218	31.57	68.694	0.78	0.816
	11.5	31.81	29.99	55.154	1.29	0.178	27.93	43.362	1.64	0.037	31.65	69.526	1.03	0.465

		T_R = 1033 Full PB (Idriss & Boulanger)				T_R = 475 Full PB (Idriss & Boulanger)				T_R = 2475 Full PB (Idriss & Boulanger)			
	Depth (m)	$N_{1,60,cs}$ site	N_{req}	$\%CSR^{site}$	FS_L	P_L	N_{req}	$\%CSR^{site}$	FS_L	P_L	N_{req}	$\%CSR^{site}$	FS_L	P_L
Santa Monica	2.5	13.78	24.77	32.419	0.51	0.992	21.24	25.278	0.66	0.934	27.6	41.896	0.40	1.000
	3.5	15.62	26.46	37.492	0.49	0.995	23.34	29.092	0.63	0.951	28.94	48.504	0.38	1.000
	4.5	16.95	27.43	41.178	0.48	0.996	24.53	31.808	0.62	0.957	29.75	53.497	0.37	1.000
	5.5	19.87	28.02	43.778	0.53	0.989	25.28	33.799	0.69	0.911	30.28	57.281	0.41	0.999
	6.5	21.47	28.47	45.978	0.56	0.982	25.78	35.272	0.73	0.875	30.65	60.207	0.43	0.999
	7.5	23.12	28.76	47.507	0.60	0.966	26.13	36.382	0.79	0.806	30.89	62.245	0.46	0.997
	8.5	24.83	28.97	48.674	0.67	0.927	26.38	37.217	0.88	0.685	31.08	63.942	0.51	0.993
	9.5	27.79	29.13	49.598	0.86	0.705	26.55	37.807	1.13	0.329	31.24	65.432	0.65	0.938
	10.5	29.76	29.24	50.252	1.06	0.410	26.65	38.163	1.40	0.111	31.35	66.490	0.81	0.783
	11.5	31.81	29.32	50.737	1.40	0.110	26.71	38.379	1.86	0.013	31.43	67.278	1.06	0.418
Seattle	2.5	13.78	24.06	30.676	0.54	0.986	19.42	22.663	0.73	0.867	27.4	41.053	0.41	0.999
	3.5	15.62	25.87	35.551	0.52	0.991	21.72	26.061	0.71	0.896	28.82	47.835	0.38	1.000
	4.5	16.95	26.92	39.157	0.50	0.993	23.04	28.479	0.69	0.907	29.67	52.963	0.37	1.000
	5.5	19.87	27.61	41.939	0.55	0.983	23.88	30.264	0.77	0.829	30.24	56.979	0.41	0.999
	6.5	21.47	28.09	44.107	0.58	0.975	24.45	31.609	0.81	0.775	30.66	60.290	0.43	0.999
	7.5	23.12	28.45	45.876	0.62	0.956	24.84	32.602	0.88	0.680	30.96	62.861	0.46	0.998
	8.5	24.83	28.72	47.291	0.69	0.911	25.11	33.326	0.98	0.533	31.22	65.243	0.50	0.994
	9.5	27.79	28.92	48.391	0.88	0.673	25.3	33.856	1.26	0.200	31.43	67.278	0.64	0.949
	10.5	29.76	29.09	49.364	1.08	0.385	25.43	34.228	1.56	0.053	31.6	69.004	0.78	0.820
	11.5	31.81	29.22	50.132	1.42	0.102	25.5	34.432	2.07	0.004	31.73	70.374	1.01	0.482